

2017

Insights Into Chromatin Modification and FANCD2 Phosphorylation in DNA Damage Repair

David Vierra II
University of Rhode Island, vierra.david@gmail.com

Follow this and additional works at: https://digitalcommons.uri.edu/oa_diss

Terms of Use

All rights reserved under copyright.

Recommended Citation

Vierra, David II, "Insights Into Chromatin Modification and FANCD2 Phosphorylation in DNA Damage Repair" (2017). *Open Access Dissertations*. Paper 660.
https://digitalcommons.uri.edu/oa_diss/660

This Dissertation is brought to you by the University of Rhode Island. It has been accepted for inclusion in Open Access Dissertations by an authorized administrator of DigitalCommons@URI. For more information, please contact digitalcommons-group@uri.edu. For permission to reuse copyrighted content, contact the author directly.

INSIGHTS INTO CHROMATIN MODIFICATION AND
FANCD2 PHOSPHORYLATION IN DNA DAMAGE REPAIR

BY

DAVID VIERRA II

A DISSERTATION SUBMITTED IN PARTIAL FULFILLMENT OF THE
REQUIREMENTS FOR THE DEGREE OF
DOCTOR OF PHILOSOPHY
IN
CELL AND MOLECULAR BIOLOGY

UNIVERSITY OF RHODE ISLAND

2017

DOCTOR OF PHILOSOPHY DISSERTATION

OF

David A Vierra II

APPROVED:

Dissertation Committee:

Major Professor Niall Howlett

Bethany Jenkins

Brenton DeBoef

Steven Q. Irvine

Nasser H. Zawia
DEAN OF GRADUATE SCHOOL

UNIVERSITY OF RHODE ISLAND
2017

Abstract

Fanconi Anemia (FA) is a rare autosomal X-linked recessive disorder, characterized by congenital abnormalities, pediatric bone marrow failure and cancer susceptibility. FA is caused by biallelic mutation in any one of 22 different genes. The main functions of the FA-BRCA pathway is the resolution of interstrand crosslinks (ICLs) within the DNA. The main activating step of the pathway is the monoubiquitination of the proteins FANCD2 and FANCI. In the first chapter of this dissertation I discuss how methylation and acetylation affect chromatin architecture and activation of the pathway. In the second chapter I will discuss the effects of FANCD2 phosphorylation in a DNA damage-independent, cell cycle-dependent manner. We show that monoubiquitination of FANCD2 is blocked by phosphorylation and that this phosphorylation acts as a molecular switch to alter FANCD2 function.

Acknowledgements

I would like to thank my committee for all their help in preparing this manuscript and for their guidance. I want express my gratitude toward my PI Dr.Howlett. His constant patience, guidance and support have made me grow as a scientist and reach a level I never thought possible. I also owe gratitude to my lab mates, who put up with my questions, jokes and over all foolishness. My greatest thanks go out to my family. Their support is what got me through this. Thanks to my parents for letting me vent to them and for supporting me no matter how stressed I got. I am so proud and lucky to have you both as parents.

PREFACE

The following dissertation has been prepared in manuscript format. Chapter 1, “Modulation of the fanconi anemia pathway via chemically induced changes in chromatin structure”, was published in *Oncotarget* and explores how chromatin state is a key determinant in DNA, in particular changes that occur due to histone post translational modifications . Chapter 2, “Phosphorylation of FANCD2 regulates its function in DNA damage independent manner” is ongoing research. This chapter presents work in which we identified a putative CDK cluster proximal to the site of monoubiquitination.

TABLE OF CONTENTS

ABSTRACT ii

ACKNOWLEDGEMENTS iii

PREFACE iv

TABLE OF CONTENTSv

LIST OF FIGURESvi

MANUSCRIPT I1

 Modulation of the Fanconi anemia pathway via chemically induced changes in
 chromatin structure 2

MANUSCRIPT II 48

 Phosphorylation of FANCD2 regulates its function in DNA damage
 independent manner 49

APENDICES 87

 CONCLUSION87

 A DUB-less step? Tighten up D-loop149

 SUPPLEMENTAL INFORMATION FOR MANUSCRIPT I162

LIST OF FIGURES

MANUSCRIPT I

FIGURE	PAGE
Figure 1. The HMTi BRD4770 induces the monoubiquitination of FANCD2 and FANCI.....	6
Figure 2 The HMTi BRD4770 induces FANCD2 chromatin localization and nuclear foci formation.....	9
Figure 3. Figure 3: BRD4770-induced activation of the FA pathway does not occur <i>via</i> the direct induction of DNA damage or altered cell cycle progression.....	12
Figure 4: BRD4770-induced activation of the FA pathway may occur <i>via</i> inhibition of the PRC2 complex	16
Figure 5: Activation of FANCD2 monoubiquitination following treatment with the EZH2 inhibitor EPZ-6438.....	20
Figure 6: Inhibition of class I and II HDACs attenuates FANCD2 and FANCI monoubiquitination in BJ-TERT cells	23
Figure 7: Inhibition of class I and II HDACs attenuates FANCD2 nuclear foci formation	26
Figure 8: Inhibition of class I and II HDACs sensitizes cells to the cytotoxic effects of mitomycin C	29

MANUSCRIPT II

FIGURE	PAGE
Figure 1. FANCD2 is monoubiquitinated in a DNA damage independent cell cycle dependent manner	53
Figure 2. FANCD2 is a potential substrate of CDK phosphorylation	56
Figure 3. FANCD2 contains a conserved putative CDK consensus site cluster.....	59
Figure 4. Mutation of the FANCD2 CDK cluster alters both FANCD2 and FANCI foci formation.....	62
Figure 5. The phospho-dead TA mutant has a high concentration of chromosomal aberrations	65
Figure 6. Phosphorylation of FANCD2 facilitates fork restart and stability	69
Figure 7. A model of the effects of FANCD2 phosphorylation.....	75

APPENDIX I

FIGURE	PAGE
Conclusion	88
Figure 1. Speculative schematic of the role of the USP1-UAF1-RAD51AP1 complex in HR	92

APPENDIX II

FIGURE	PAGE
Supplementary Figure 1: The HMTi BRD4770 induces FANCD2 nuclear foci formation.....	99
Supplementary Figure 2: BRD4770-induced activation of the FA pathway does not occur <i>via</i> the direct induction of DNA damage	101
Supplementary Figure 3: BRD4770-induced activation of the FA pathway may occur <i>via</i> inhibition of the PRC2 complex.....	103
Supplementary Figure 4: Activation of FANCD2 monoubiquitination following treatment with the EZH2 inhibitor EPZ-6438.....	106
Supplementary Figure 5: Activation of FANCD2 monoubiquitination following treatment with the EZH2 inhibitor EPZ-6438.....	108

Manuscript I

Published in Oncotarget

Modulation of the fanconi anemia pathway via chemically induced changes in chromatin structure

David A. Vierra¹, Jada L. Garzon¹, Meghan A. Rego², Morganne M. Adroved¹, Maurizio Mauro³ and Niall G. Howlett¹

¹ Department of Cell and Molecular Biology, University of Rhode Island, Kingston, Rhode Island, U.S.A

² Addgene, Cambridge, Massachusetts, U.S.A

³ Department of Obstetrics & Gynecology and Women's Health, Albert Einstein College of Medicine, New York, New York, U.S.A

¹Corresponding author: Niall G. Howlett Ph.D., 379 Center for Biotechnology and Life Sciences, 120 Flagg Road, Kingston, RI, USA, Tel.: +1 401 874 4306; Fax: +1 401 874 2065; *Email address:* nhowlett@uri.edu

Keywords: fanconi anemia, FANCD2, FANCI, monoubiquitination, histone methylation

Fanconi anemia (FA) is a rare disease characterized by congenital defects, bone marrow failure, and atypically early-onset cancers. The FA proteins function cooperatively to repair DNA interstrand crosslinks. A major step in the activation of the pathway is the monoubiquitination of the FANCD2 and FANCI proteins, and their recruitment to chromatin-associated nuclear foci. The regulation and function of FANCD2 and FANCI, however, is poorly understood. In addition, how chromatin state impacts pathway activation is also unknown. In this study, we have examined the influence of chromatin state on the activation of the FA pathway. We describe potent activation of FANCD2 and FANCI monoubiquitination and nuclear foci formation following treatment of cells with the histone methyltransferase inhibitor BRD4770. BRD4770-induced activation of the pathway does not occur via the direct induction of DNA damage or via the inhibition of the G9a histone methyltransferase, a mechanism previously proposed for this molecule. Instead, we show that BRD4770- inducible FANCD2 and FANCI monoubiquitination and nuclear foci formation may be a consequence of inhibition of the PRC2/EZH2 chromatin-modifying complex. In addition, we show that inhibition of the class I and II histone deacetylases leads to attenuated FANCD2 and FANCI monoubiquitination and nuclear foci formation. Our studies establish that chromatin state is a major determinant of the activation of the FA pathway and suggest an important role for the PRC2/EZH2 complex in the regulation of this critical tumor suppressor pathway.

INTRODUCTION

All organisms are continuously exposed to endogenous and exogenous DNA damaging agents, including reactive oxygen species and aldehydes from normal metabolic processes and UV irradiation from sunlight. The timely and accurate repair of DNA damage is essential for the maintenance of genome stability and organismal survival. As a consequence, prokaryotic and eukaryotic organisms have evolved complex and highly orchestrated DNA repair pathways to effectively repair damaged DNA. Chromatin represents the higher order macromolecular complex of DNA and histone proteins, and chromatin plasticity has become increasingly recognized as a major determinant of DNA damage recognition, signaling, and repair [1–3]. The nucleosome is the fundamental subunit of chromatin and exhibits plasticity via compositional alteration, translational repositioning, and the posttranslational modification of histone tails. Histone tails are subject to a wide variety of posttranslational modifications including acetylation, methylation, phosphorylation, and ubiquitination [4]. Histone acetylation homeostasis is mediated by histone acetyltransferases (HATs), e.g. TIP60/KAT5, and deacetylases (HDACs), e.g. HDAC1 and HDAC2. Underscoring the importance of histone acetylation in DNA repair, key roles for TIP60/KAT5, HDAC1, and HDAC2 in the maintenance of genome stability have been established [5–7].

Fanconi anemia (FA) is a rare autosomal and X-linked genetic disease characterized by congenital defects, bone marrow failure, and increased cancer risk in early adulthood [8]. FA is caused by mutation of any one of 21 genes. The FA proteins function primarily in the repair of DNA interstrand crosslinks (ICLs), lesions that block the replication and transcription machineries, which lead to structural and numerical

chromosome aberrations if repaired erroneously [8–11]. A central step in the activation of the FA pathway is the site-specific monoubiquitination of the FANCD2 and FANCI proteins [12–14]. Monoubiquitinated FANCD2 and FANCI localize to discrete sites within chromatin where they are hypothesized to promote the recruitment of several structure-specific endonucleases, including FAN1 (FANCD2-associated nuclease 1) and FANCD1/ERCC1 [15–18]. While FANCD2 and FANCI function primarily within chromatin, the contribution of chromatin plasticity, and specifically, the effects of changes in histone tail post translational modifications, on their activation and function have yet to be determined. Furthermore, while chromatin remodeling at DNA double-strand breaks (DSBs) has been extensively studied [1–3], very little is known about the role of chromatin remodeling in the context of ICL repair.

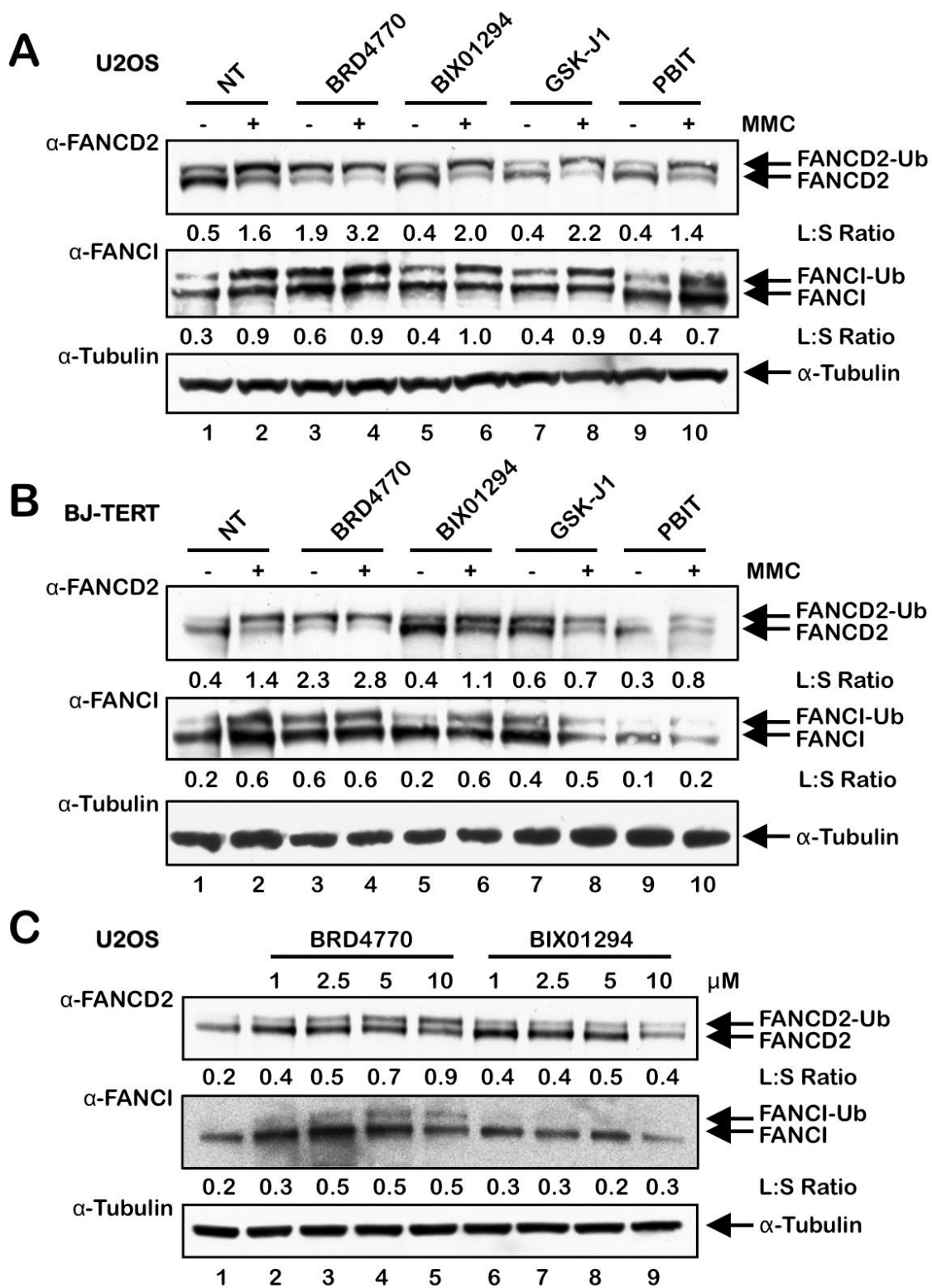
In this study we have examined the influence of chromatin structure on the activation of the FA pathway. Specifically, we have examined the effects of several histone methyltransferase (HMT), demethylase (HDM), and deacetylase (HDAC) inhibitors on FANCD2 and FANCI monoubiquitination and their assembly into discrete nuclear foci. We describe potent activation of FANCD2 and FANCI monoubiquitination in chromatin, and enhanced FANCD2 and FANCI nuclear foci formation, following cellular exposure to the HMT inhibitor BRD4770. BRD4770-induced activation of the pathway does not appear to occur via the direct induction of DNA damage per se, or via the inhibition of the G9a histone methyltransferase, a mechanism previously proposed for this molecule [19]. In contrast, our results suggest that BRD4770-induced activation of the pathway may be a consequence of inhibition of PRC2 (Polycomb Repressive Complex 2) and, specifically, its catalytic HMT EZH2. In addition, we demonstrate that

inhibition of class I and II HDACs with trichostatin A (TSA) and vorinostat (SAHA) leads to attenuated ICL-inducible FANCD2 and FANCI monoubiquitination and nuclear foci formation. Our results establish that chromatin plasticity, and in particular the posttranslational modification of histone tails, is a critical determinant in the activation of the FA tumor suppressor pathway.

RESULTS

Activation of FANCD2 and FANCI monoubiquitination by the HMTi BRD4770. To explore the effects of global alterations in histone methylation on the activation of the FA pathway, we exposed the transformed osteosarcoma cell line U2OS and the nontransformed telomerase (hTERT)- immortalized line BJ-TERT to the HMT inhibitors (HMTi) BRD4770 and BIX01294 and the HDM inhibitors (HDMi) GSK-J1 and PBIT, and examined FANCD2 and FANCI monoubiquitination. BRD4770 is a S-adenosylmethionine (SAM) mimetic and competitive inhibitor of PRC2/ EZH2 and G9a [19–21]. BIX01294 is a non-SAM mimetic selective inhibitor of G9a [21]. Treatment with BRD4770 resulted in a marked increase in FANCD2 and FANCI monoubiquitination in both U2OS and BJTERT cells, even in the absence of the ICL-inducing agent mitomycin C (MMC) (Figure 1A and B, lane 3). Indeed, the ratio of FANCD2-Ub to FANCD2 (L:S ratio) was higher in cells treated with BRD4770 alone than in cells treated with MMC alone (Figure 1A and B, compare lanes 2 and 3). BRD4770-induced activation of FANCD2 monoubiquitination also occurred in a concentration-dependent manner (Figure 1C). In contrast, no major

Figure 1: The HMTi BRD4770 induces the monoubiquitination of FANCD2 and FANCI. (A) and (B), U2OS (A) and BJ-TERT (B) cells were incubated in the absence (NT) or presence of 10 μ M BRD4770, 2.5 μ M BIX01294, 5 μ M GSK-J1 and 1 μ M PBIT, with (+) and without (-) 200 nM mitomycin C (MMC) for 24 h. Whole-cell lysates were prepared and immunoblotted with anti-FANCD2, anti-FANCI, and anti- α -Tubulin antibodies. (C) U2OS cells were incubated with the indicated concentrations of BRD4770 and BIX01294 for 24 h, and whole-cell lysates were immunoblotted with anti-FANCD2, anti-FANCI, and anti- α -Tubulin antibodies. L:S Ratio, ratio of monoubiquitinated to nonubiquitinated FANCD2.

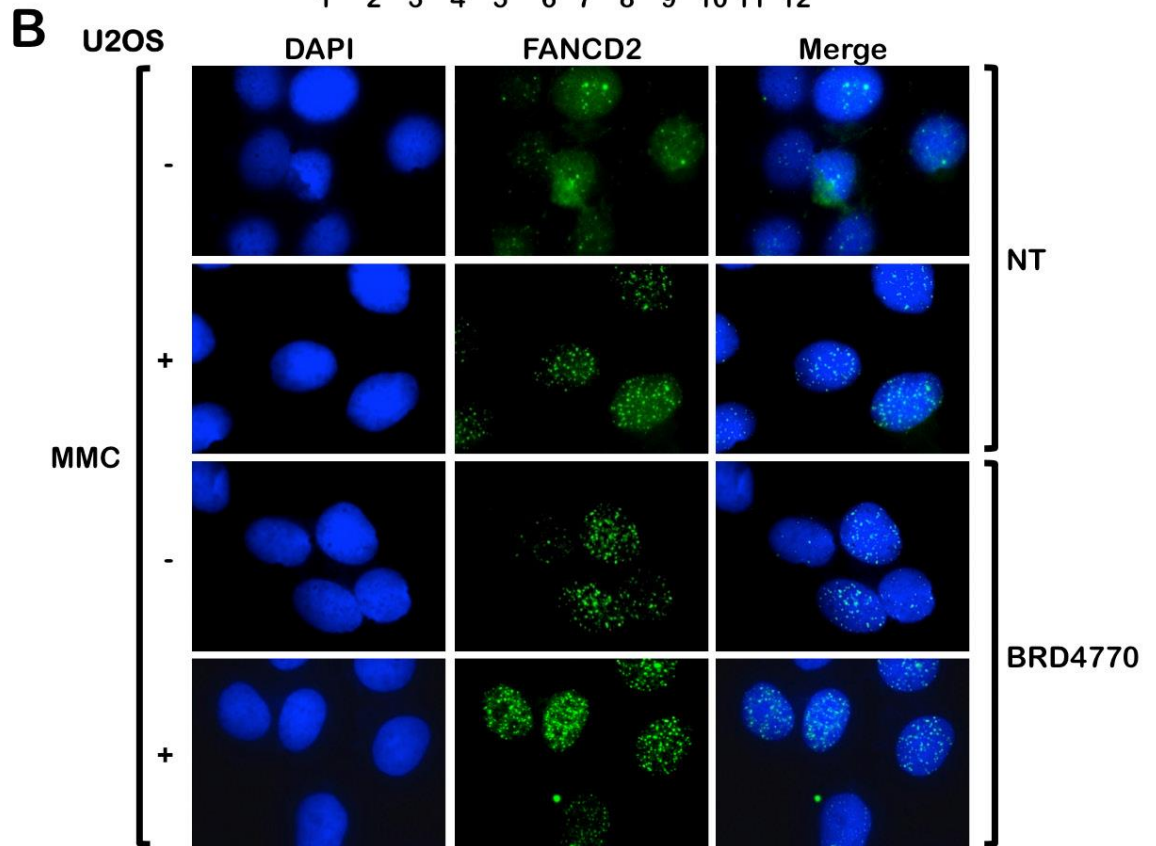
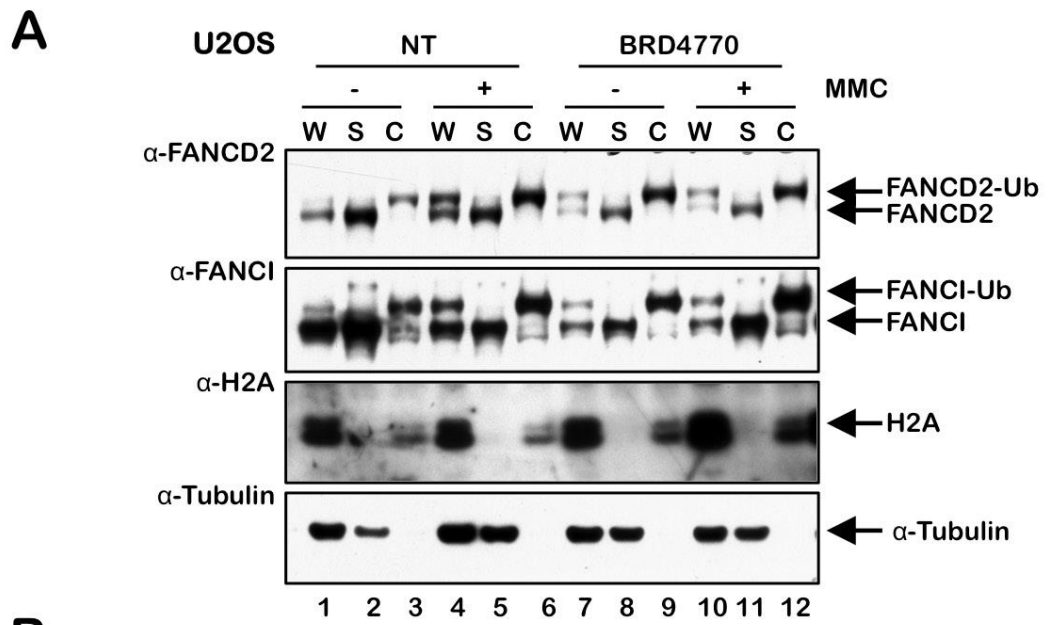


effects on levels of spontaneous or ICL-inducible FANCD2/I monoubiquitination were observed for the other inhibitors tested, other than a slight increase in the FANCD2/I L:S ratios following treatment of BJ-TERT cells with GSK-J1 (Figure 1B).

BRD4770 promotes FANCD2 chromatin localization and nuclear foci formation.

Next, we examined the effects of BRD4770 treatment on the localization of FANCD2 to chromatin and its assembly into nuclear foci. Cells were incubated in the absence or presence of BRD4770, both with and without MMC, and whole-cell (W), soluble cytoplasmic and nuclear (S), and chromatin-enriched (C) protein lysates were prepared and analyzed by immunoblotting. We observed greatly elevated levels of monoubiquitinated FANCD2 and FANCI in the chromatin fraction of cells treated with BRD4770 alone (Figure 2A, compare lanes 3 and 9). In addition, using immunofluorescence microscopy (IF), we analyzed FANCD2 nuclear foci formation, an indicator of the localization of FANCD2 to sites of damaged DNA in chromatin [12, 22], following treatment with BRD4770 alone and following combined treatment with BRD4770 and MMC. We observed a striking increase in the percentage of nuclei exhibiting greater than 5 FANCD2 foci in both U2OS and BJTERT cells following BRD4770 treatment (Figure 2B and Supplementary Figure 1A and B). Levels of FANCD2 nuclear foci formation in cells treated with BRD4770 alone were comparable to that observed following MMC treatment (Supplementary Figure 1A and B). These results identify BRD4770 as a major inducer of FANCD2 monoubiquitination and nuclear foci formation and strongly suggest that changes in histone methylation status are a critical determinant in the activation of the FA

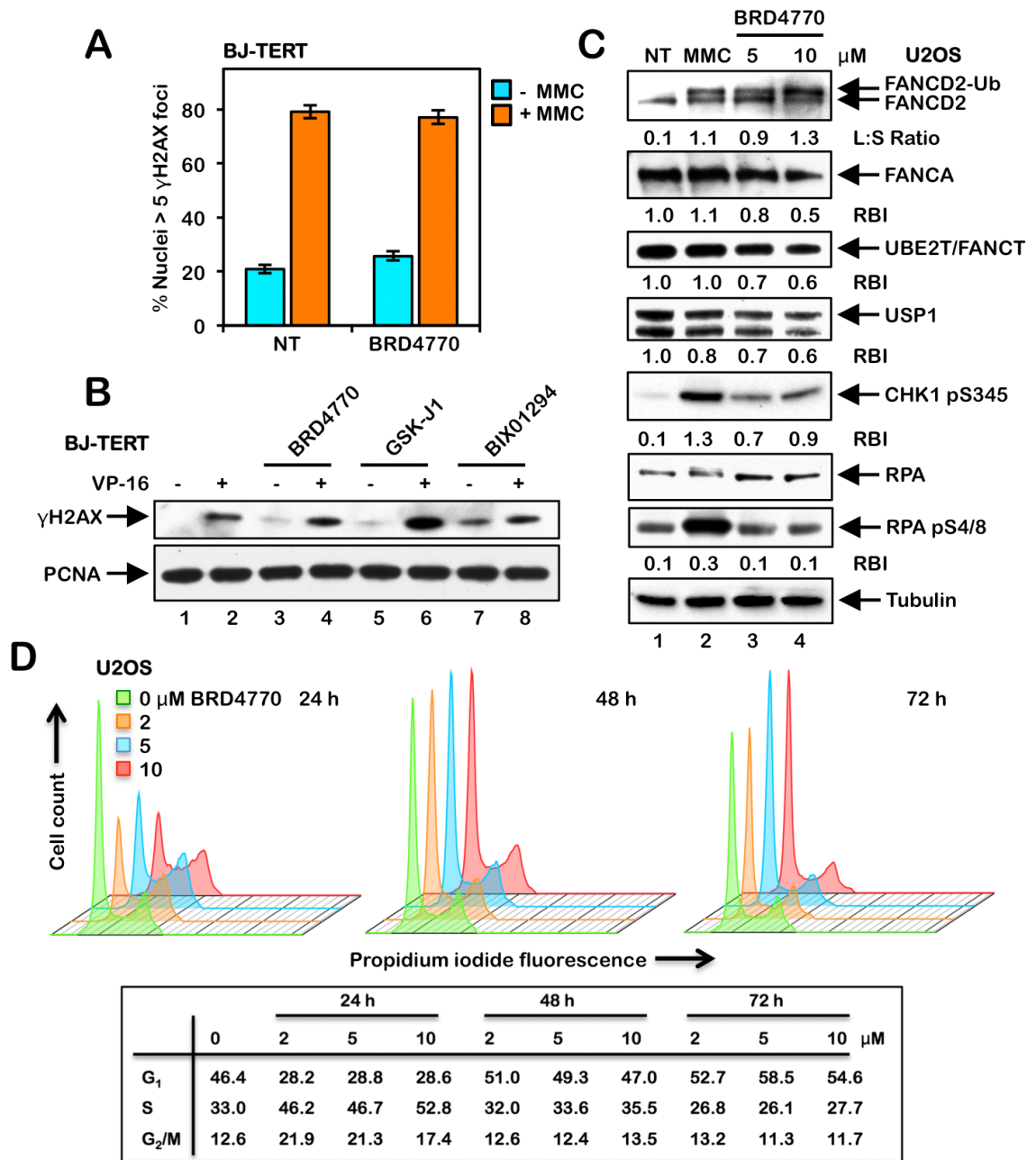
Figure 2: The HMTi BRD4770 induces FANCD2 chromatin localization and nuclear foci formation. (A) U2OS cells were incubated in the absence (NT) or presence of 10 μ M BRD4770 with (+) and without (-) 200 nM mitomycin C (MMC) for 24 h. Whole-cell lysates (W) and soluble nuclear and cytoplasmic (S) and chromatin-enriched (C) fractions were prepared and immunoblotted with anti-FANCD2, anti-FANCI, anti-H2A, and anti- α -Tubulin antibodies. (B) U2OS cells were incubated with (+) and without (-) 200 nM MMC in the absence (NT) or presence of 10 μ M BRD4770 for 24 h. Cells were fixed and stained with rabbit polyclonal anti-FANCD2 antibody (green) and counterstained with DAPI (blue), and the number of nuclei with >5 FANCD2 foci were scored. At least 300 nuclei were scored for each treatment. Representative immunofluorescence microscopy images are shown.



pathway. Consistent with BRD4770 functioning via the modification of chromatin structure, we observed a distinct change in the staining pattern of the heterochromatin marker HP1 α following BRD4770 treatment (Supplementary Figure 1C).

BRD4770-inducible activation of the FA pathway does not occur via direct induction of DNA damage, increased expression of the FA core complex, or changes in cell cycle progression. One possible explanation for BRD4770-induced activation of FANCD2 and FANCI monoubiquitination and nuclear foci formation is that BRD4770 induces DNA damage directly. To test this hypothesis, we examined levels of the phosphorylated H2A variant H2AX (γ H2AX), a well-established biomarker of DNA DSB formation [23], in cells treated with and without BRD4770. No differences in the number of nuclei exhibiting γ H2AX foci were observed between untreated cells and cells treated with BRD4770, both in the absence or presence of MMC (Figure 3A and Supplementary Figure 2). Similar results were observed in both U2OS and BJ-TERT cells (Figure 3A and Supplementary Figure 2). U2OS cells have a highly unstable karyotype, with recurrent breakage-fusion-bridge cycles most likely contributing to the elevated spontaneous levels of γ H2AX nuclear foci formation observed in these cells (Supplementary Figure 2). While we observed a faint γ H2AX signal for cells treated with BRD4770 alone *via* immunoblotting, this level was markedly lower than that observed following exposure to the topoisomerase type II inhibitor etoposide (VP-16), a well known inducer of DNA DSBs, and no different to that observed following GSK-J1 treatment (Figure 3B). We also examined levels of RPA S4/8 phosphorylation, a marker of single-stranded DNA [24], following BRD4770 exposure. While MMC treatment led to a strong increase in levels of RPA

Figure 3: BRD4770-induced activation of the FA pathway does not occur *via* the direct induction of DNA damage or altered cell cycle progression. (A) BJ-TERT cells were incubated with (+) and without (-) 200 nM mitomycin C (MMC) in the absence (NT) or presence of 10 μ M BRD4770 for 24 h. Cells were fixed and stained with mouse monoclonal anti- γ H2AX antibody and counterstained with DAPI, and the number of nuclei with >5 γ H2AX foci were scored. At least 300 nuclei were scored for each treatment and this experiment was performed three times with similar results. Error bars represent the standard errors of the means from three independent experiments. (B) BJ-TERT cells were incubated with (+) and without (-) 0.4 μ M etoposide (VP-16), in the absence or presence of 10 μ M BRD4770, 5 μ M GSK-J1 and 2.5 μ M BIX01294, for 24 h. Whole-cell lysates were immunoblotted with anti- γ H2AX and anti-PCNA (loading control) antibodies. (C) U2OS cells were incubated in the absence (NT) or presence of 200 nM MMC or 5 and 10 μ M BRD4770 for 24 h. Whole-cell lysates were prepared and immunoblotted with anti-FANCD2, anti-FANCA, anti-UBE2T, anti-USP1, anti-CHK1 pS345, anti-RPA, anti-RPA pS4/8, and anti- α -Tubulin antibodies. L:S Ratio, ratio of monoubiquitinated to nonubiquitinated FANCD2; RBI, relative band intensity. (D) U2OS cells were incubated in the absence or presence of 2, 5, and 10 μ M BRD4770 for 24, 48, or 72 h. Cells were fixed in ice-cold ethanol, stained with propidium iodide, and analyzed by flow cytometry. Cell cycle stage distributions were determined using FlowJo v10.2.

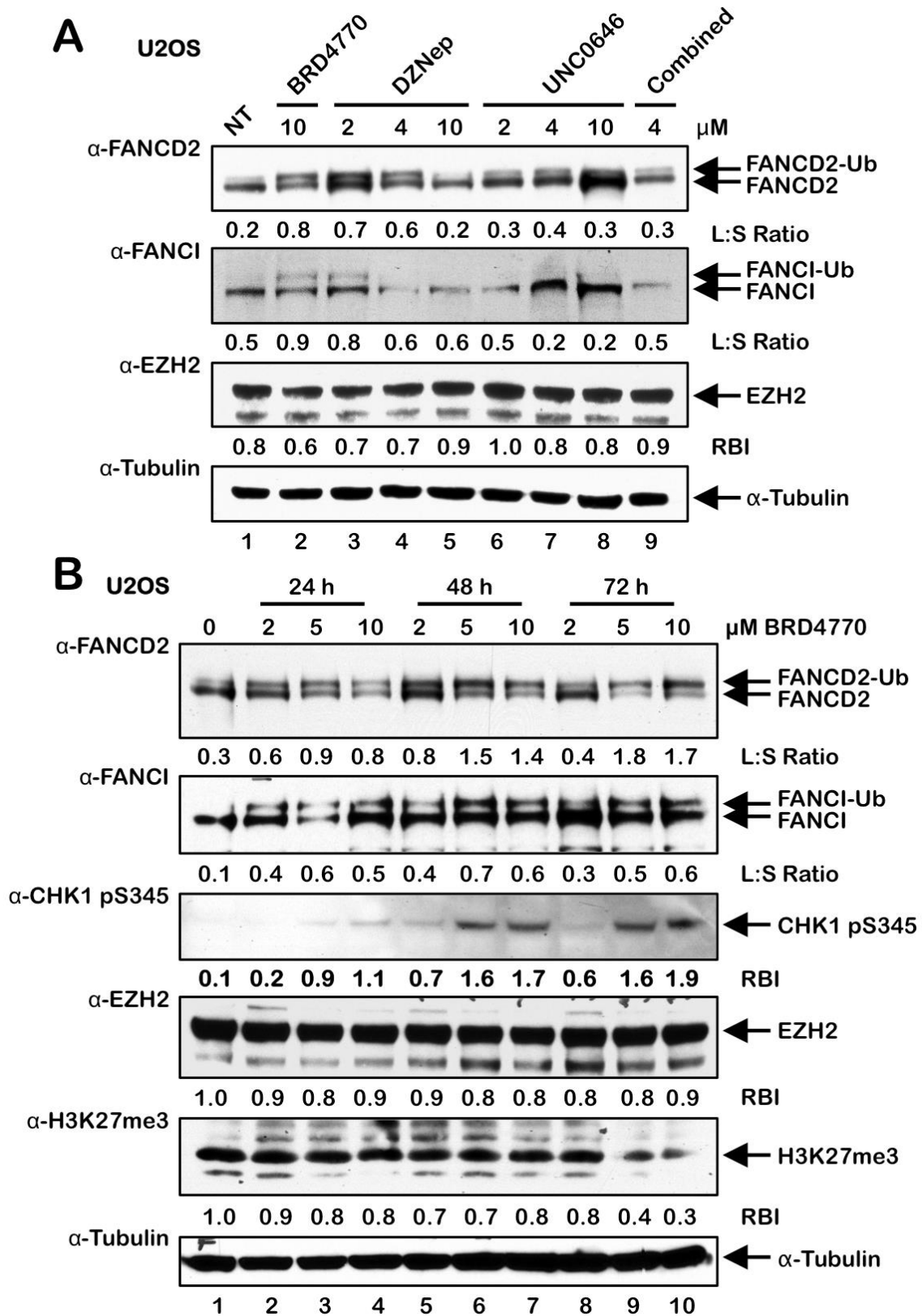


pS4/8, no increase in levels above that of untreated cells was observed for BRD4770 (Figure 3C). We also examined the effects of BRD4770 treatment on levels of the FA core complex proteins FANCA and UBE2T/FANCT. UBE2T/FANCT is the FANCD2 E2 ubiquitin-conjugating enzyme [25]. Levels of both proteins decreased following BRD4770 treatment (Figure 3C). Decreased levels of FANCA were also observed following exposure of HCT116 p53^{+/+} and p53^{-/-} cells to BRD4770 (see Supplementary Figure 3D). Similarly, we observed a reduction in levels of the USP1 de-ubiquitinating enzyme following BRD4770 treatment (Figure 3C). Concomitant reductions in the levels of FANCA, UBE2T/FANCT, and USP1 cannot explain the observed BRD4770-induced FANCD2 and FANCI monoubiquitination and nuclear foci formation.

We observed an increase in levels of phosphorylated CHK1 S345 following treatment with BRD4770, albeit to a lesser extent than that observed following MMC treatment (Figure 3C). Finally, we examined the effects of BRD4770 treatment on cell cycle progression. Following exposure to BRD4770 for 24 h, we observed an increase in the percentage of cells in S-phase at all concentrations of BRD4770 examined (Figure 3D). However, following exposure to BRD4770 for 48 and 72 h, where maximal induction of FANCD2 and FANCI monoubiquitination was observed (see Figure 4B), the cell cycle stage profiles did not differ substantially from that of untreated cells (Figure 3D). Taken together, these results argue that BRD4770-induced activation of the FA pathway does not appear to be a consequence of direct induction of DNA damage, alterations in expression of the FANCD2 core monoubiquitination proteins, or major changes to cell cycle progression.

BRD4770-induced activation of the FA pathway may occur *via* inhibition of the PRC2 complex BRD4770 is a SAM mimetic and a structural analogue of BIX01338, a non-selective HMT inhibitor with similar IC₅₀ values against the G9a and SUV39H1 HMTs [19–21]. Therefore, we next treated U2OS cells with varying concentrations of BIX01338 to determine if we would observe activation of the FA pathway, similar to that observed for BRD4770. Surprisingly, we did not observe any appreciable induction of FANCD2 or FANCI monoubiquitination following treatment with BIX01338 for acute (24 h) (Supplementary Figure 3A) or extended periods (up to 10 d) (results not shown). BRD4770 is a methyl ester analogue of BRD9539, and previous experiments with BRD9539 have shown that it exhibits specificity for G9a and PRC2 (Polycomb Repressive Complex 2) [19]. EZH2 is the catalytic HMT of PRC2, and catalyzes the deposition of the transcriptionally repressive mark H3K27me₃ [26]. Therefore, to determine if BRD4770-induced activation of FANCD2 monoubiquitination might be a specific consequence of G9a and/or EZH2 inhibition, we treated cells with the DZNep and UNC0646 HMT inhibitors: DZNep treatment has been reported to lead to cellular depletion of EZH2 [27], while UNC0646 is a potent inhibitor of G9a [28]. We observed modest induction of FANCD2 and FANCI monoubiquitination following exposure to 2 and 4 μM DZNep (Figure 4A). Considerable cell toxicity was observed at 10 μM DZNep (results not shown). Under these conditions, we did not observe a decrease in levels of EZH2 expression. However, reduced levels of EZH2 were observed following incubation with DZNep, and BRD4770 to a lesser extent, for 4 and 8 days (Supplementary Figure 3B). In contrast to DZNep, no induction of FANCD2/I monoubiquitination was observed

Figure 4: BRD4770-induced activation of the FA pathway may occur *via* inhibition of the PRC2 complex. (A) U2OS cells were incubated in the absence (NT) or presence of BRD4770, DZNep, UNC0646, and DZNep and UNC0646 combined (4 μ M each) for 24 h. Whole-cell lysates were prepared and immunoblotted with anti-FANCD2, anti-FANCI, anti-EZH2, and anti- α -Tubulin antibodies. (B) U2OS cells were incubated in the absence or presence of 2, 5, and 10 μ M BRD4770 for 24, 48, or 72 h. Whole-cell lysates were prepared and immunoblotted with anti-FANCD2, anti-FANCI, anti-CHK1 pS345, anti-EZH2, anti-H3K27me3, and anti- α -Tubulin antibodies. L:S Ratio, ratio of monoubiquitinated to nonubiquitinated FANCD2; RBI, relative band intensity.



following treatment with UNC0646, and combined DZNep/UNC0646 treatment resulted in considerable cell death (Figure 4A and results not shown). Consistent with these findings, we also observed a modest yet statistically significant increase in FANCD2 nuclear foci formation in cells treated with DZNep and not with UNC0646 (Supplementary Figure 3C). We note that the degree of DZNep-induced FANCD2/I monoubiquitination was experimentally variable, most likely a consequence of its pleiotropic nature. To further explore the potential role of EZH2 and H3K27me3 in BRD4770-inducible FANCD2/I monoubiquitination, we exposed U2OS cells to BRD4770 for 24, 48, and 72 h and examined levels of EZH2 and H3K27me3 (Figure 4B). We observed reductions in levels of H3K27me3 following treatment with higher concentrations of BRD4770 for 72 h, when induction of FANCD2 monoubiquitination was maximal (Figure 4B). Under the same conditions, we did not observe any significant reductions in EZH2 levels (Figure 4B). Similarly, we also observed a modest reduction in levels of H3K27me3 in HCT116 p53^{-/-} cells treated with BRD4770 for 24 h and a more pronounced reduction in HeLa cells treated with BRD4770 for 72 h (Supplementary Figures 3D and 3E). We again observed induction of CHK1 pS345 upon exposure to higher concentrations of BRD4770 for extended periods (Figure 4B).

EPZ-6438-mediated inhibition of PRC2/ EZH2 leads to activation of FANCD2 monoubiquitination. To further analyze the role of PRC2 and EZH2 in the activation of the FA pathway, cells were treated with EPZ-6438, an EZH2-specific inhibitor [29, 30], and FANCD2 and FANCI monoubiquitination and nuclear foci formation were analyzed. In MCF10A cells, a spontaneously-immortalized, nontransformed, mammary epithelial line, EPZ-6438 treatment led to a pronounced increase in FANCD2 and

FANCI protein levels, FANCD2 and FANCI monoubiquitination, and FANCD2 nuclear foci formation (Figure 5A and Supplementary Figure 4). Interestingly, EPZ-6438 treatment led to an increase in levels of EZH2, possibly a cellular response to chemical inhibition of EZH2, and an overall reduction in levels of H3K27me3 (Figure 5A). EPZ-6438 treatment also resulted in increased FANCD2 monoubiquitination in isogenic HCT116 p53^{+/+} and p53^{-/-} cells (Figure 5B) and HeLa cells (Figure 5C). In contrast to MCF10A, HeLa, and HCT116, we did not detect increased FANCD2 monoubiquitination in U2OS cells treated with EPZ-6438 (results not shown). Taken together, our results suggest that BRD4770-induced activation of the FA pathway may occur *via* inhibition of the PRC2 complex, and specifically EZH2 HMT activity, and a consequent decrease in levels of H3K27me3.

Inhibition of class I and II HDACs attenuates activation of the FA pathway To investigate the influence of histone acetylation state on the activation of the FA pathway, we next examined the effects of the class I and II HDAC inhibitors trichostatin A (TSA) and vorinostat (SAHA) on FANCD2 and FANCI monoubiquitination and nuclear foci formation. Interestingly, for HeLa cells, we did not observe any appreciable differences in the levels of spontaneous or ICL-inducible FANCD2 or FANCI monoubiquitination when cells were treated with TSA or SAHA (Figure 6A and 6B). In contrast, when BJ-TERT cells were treated with TSA or SAHA, we observed a marked reduction in the levels of ICL-inducible FANCD2 and FANCI monoubiquitination (Figure 6C and D). TSA and SAHA treatment led to a reduction in ICL-inducible CHK1 S345 phosphorylation in both lines examined

Figure 5: Activation of FANCD2 monoubiquitination following treatment with the EZH2 inhibitor EPZ-6438. (A-C) MCF10A (A), HCT116 p53^{+/+} and p53^{-/-} (B), and U2OS (C) cells were treated with the indicated concentrations of the EZH2-specific inhibitor EPZ-6438 for 24 h (A and B) or 24, 48, and 72 h (C). Whole-cell lysates were prepared and immunoblotted with the indicated antibodies. L.E., light exposure; D.E., dark exposure; L:S Ratio, ratio of monoubiquitinated to nonubiquitinated FANCD2; RBI, relative band intensity.

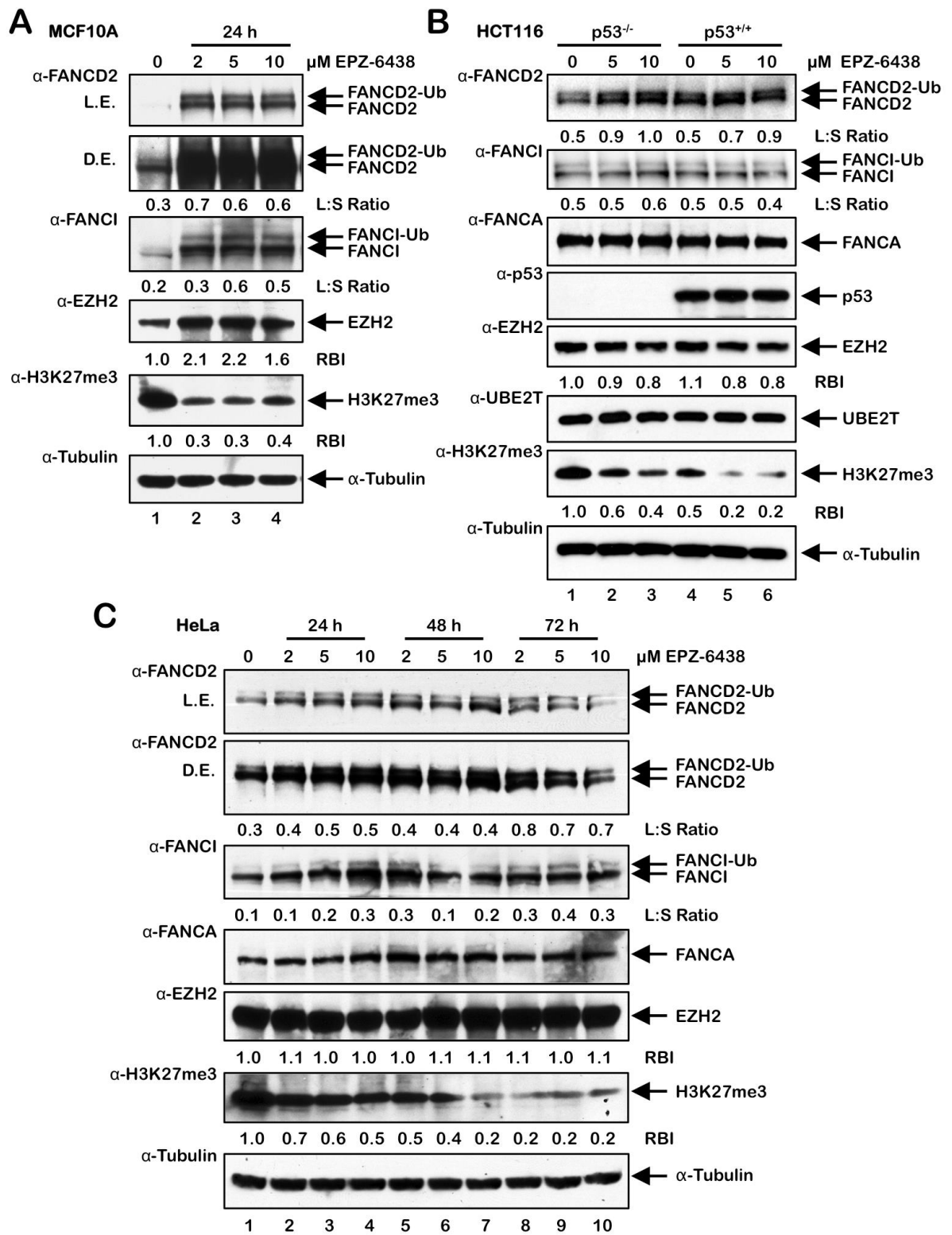
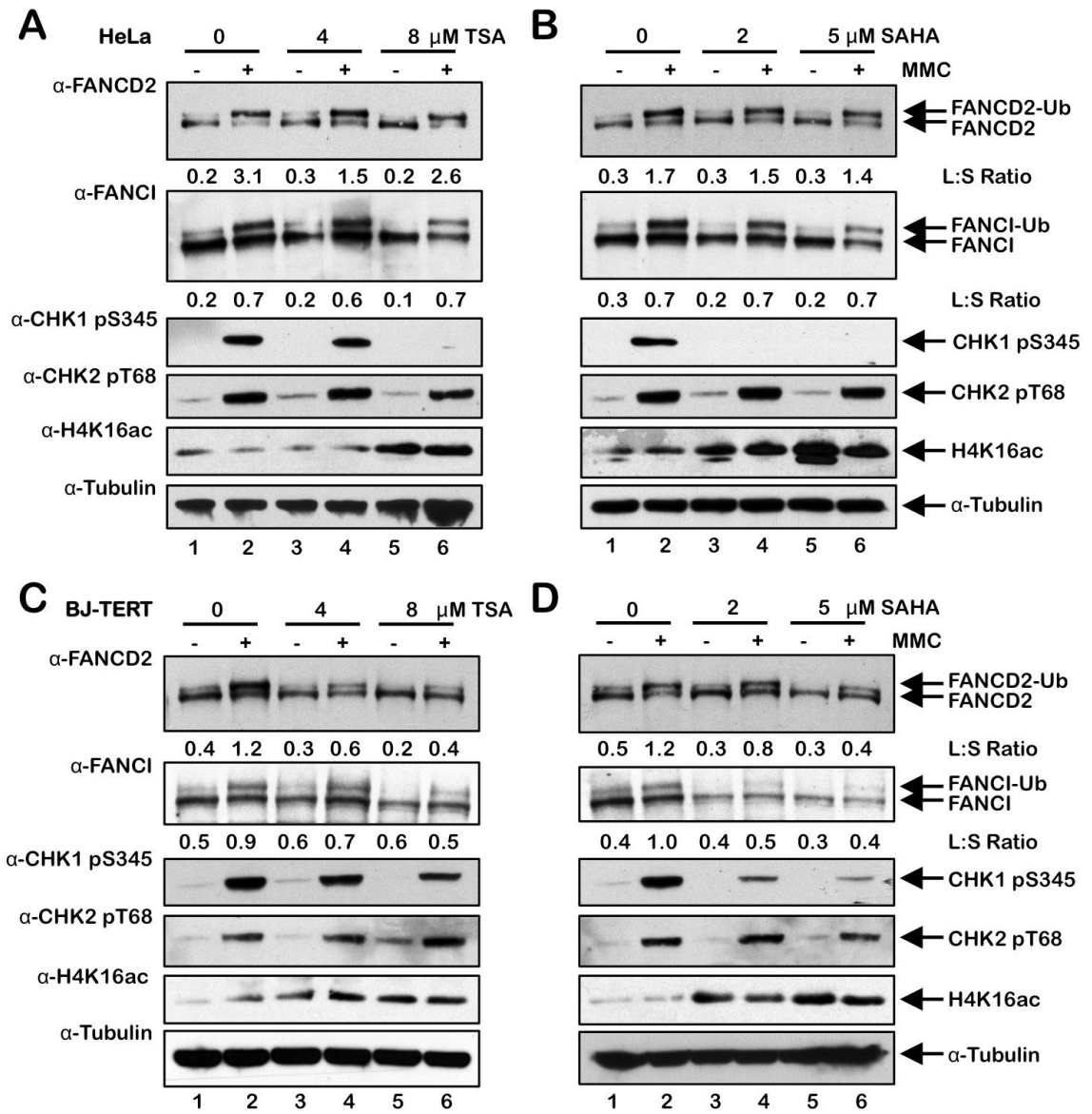


(Figure 6). In contrast, incubation with TSA and SAHA did not lead to any observable changes in levels of ICL-inducible CHK2 pT68 (Figure 6). We observed a concentration-dependent increase in the levels of H4K16ac following treatment with TSA and SAHA confirming their inhibition of histone deacetylation (Figure 6). We also observed a reduction in spontaneous and ICL-inducible FANCD2 nuclear foci formation in both HeLa and BJ-TERT cells treated with TSA or SAHA (Figure 7A–7D). Consistent with our immunoblotting results, this effect was particularly striking for BJ-TERT cells with a lesser effect observed for HeLa cells (Figure 7A–7D). The FA pathway is a major determinant of cellular sensitivity to ICL-inducing agents. Therefore we next examined if treatment with HDAC I and II inhibitors would sensitize cells to the cytotoxic effects of MMC. Indeed, even at the low concentrations of inhibitors examined, treatment with the HDAC I and II inhibitors sodium butyrate (NaB) and TSA sensitized BJ-TERT cells to the cytotoxic effects of MMC over a range of MMC concentrations (Figure 8A and B). In contrast, treatment with nicotinamide (NAM), an inhibitor of the NAD⁺ (nicotinamide adenine dinucleotide)-dependent sirtuin (class III) family of HDACs, did not impact cellular sensitivity to MMC (Figure 8C). Taken together, our results indicate that HDAC1 and HDAC2 positively regulate activation of the FA pathway and that cellular sensitivity to ICL-inducing agents, which are widely used in cancer chemotherapy, may be increased *via* HDAC1/2 inhibition.

DISCUSSION

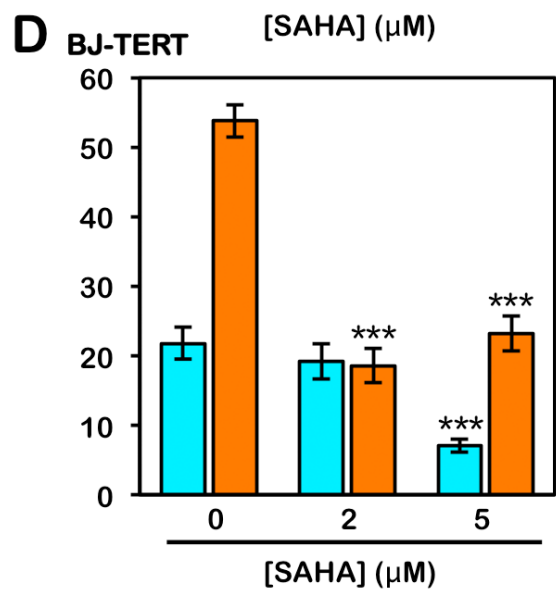
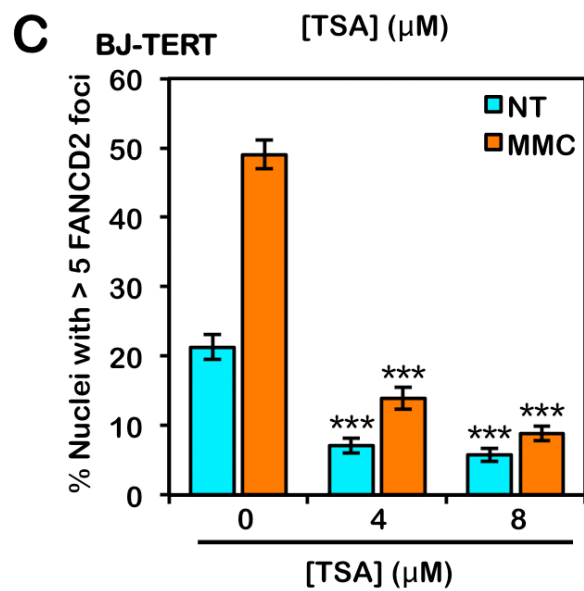
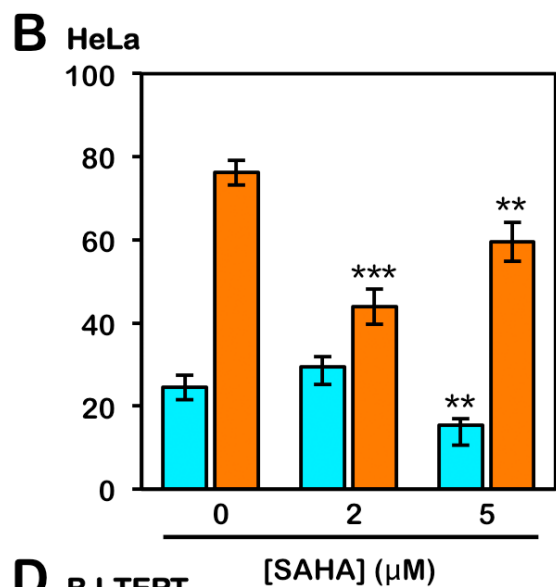
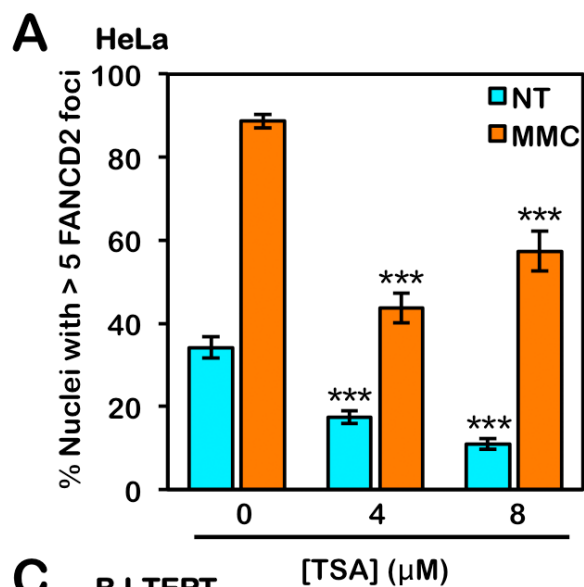
In this study, we have established that chromatin state is an important determinant in the activation of the FA pathway. Specifically, we have established that treatment with

Figure 6: Inhibition of class I and II HDACs attenuates FANCD2 and FANCI monoubiquitination in BJ-TERT cells. (A) and (B), HeLa cells were pre-treated with the indicated concentrations of trichostatin A (TSA) (A) or vorinostat (SAHA) (B) for 4 h, followed by co-incubation with (+) and without (-) 200 nM MMC for a further 20 h. Whole-cell lysates were prepared and immunoblotted with anti-FANCD2, anti-FANCI, anti-CHK1 pS345, anti-CHK2 pT68, anti-H4K16ac, and anti- α -Tubulin antibodies. (C) and (D), BJ-TERT cells were treated identically to that described for HeLa cells above. L:S Ratio, ratio of monoubiquitinated to nonubiquitinated FANCD2.



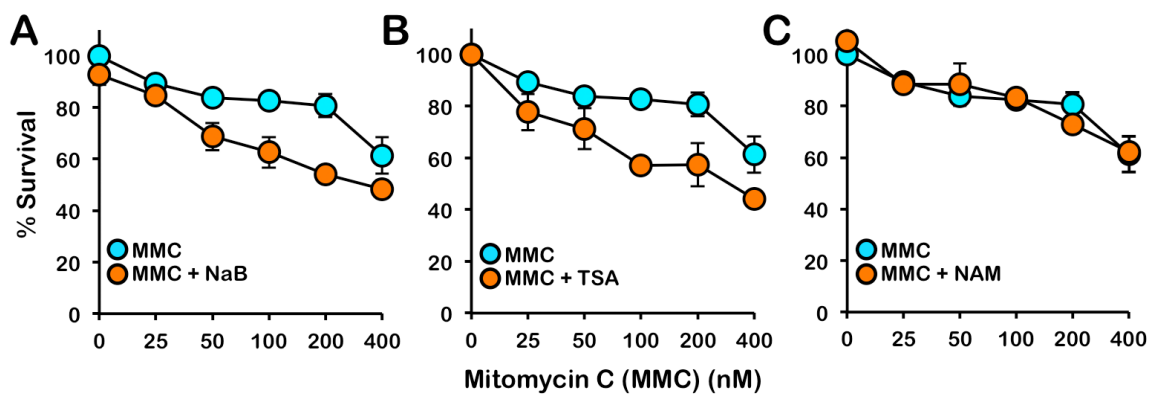
the HMTi BRD4770 and inhibition of the class I and II HDACs strongly impacts activation of the FA pathway. BRD4770 was recently discovered in a focused screen of a 2-substituted benzimidazole library [19]. While in *in vitro* biochemical assays, BRD9539, the carboxylic acid derivative of BRD4770, effectively inhibited both G9a and PRC2/EZH2 in a concentration-dependent manner, these studies concluded that BRD4770 functions primarily *via* the inhibition of G9a [19]. However, in our experiments, while BRD4770 robustly promoted FA pathway activation, several G9a-specific inhibitors - including BIX01294 and UNC0646 - failed to promote FA pathway activation. Our results suggest that BRD4770 does not act primarily *via* G9a inhibition, and that G9a does not play a significant role in the regulation of the FA pathway. Instead, our findings suggest that BRD4770 may exert its cellular effects, at least in part, *via* the inhibition of PRC2/EZH2, and that PRC2/EZH2 may play an important role in the regulation of the activation of the FA pathway. Several findings support this model: Exposure to BRD4770 resulted in reduced levels of H3K27me3 - the transcriptionally repressive mark deposited by PRC2/EZH2 [26] - in several cell models. Modest activation of FANCD2 monoubiquitination and nuclear foci formation was observed following treatment with the PRC2/EZH2 inhibitor DZNep [27]. However, while DZNep was initially reported to be selective for PRC2/EZH2 [27], as a *S*-adenosylhomocysteine hydrolase inhibitor, DZNep can also affect global histone methylation patterns [31]. This led us to examine the effects of inhibition of EZH2 with the SAM-competitive inhibitor EPZ-6438. EPZ-6438 is a potent and selective EZH2 inhibitor with an inhibition constant (K_i) of 2.5 nM. EPZ-6438 is 35-fold and >4,500-fold more selective for EZH2 than EZH1 and 14 other HMTs

Figure 7: Inhibition of class I and II HDACs attenuates FANCD2 nuclear foci formation. (A) and (B), HeLa cells were treated with the indicated concentrations of trichostatin A (TSA) (A) or vorinostat (SAHA) (B) in the absence (NT) or presence (MMC) of 200 nM mitomycin C (MMC) for 24 h. Cells were fixed and stained with rabbit polyclonal anti-FANCD2 antibody and counterstained with DAPI, and the number of nuclei with >5 FANCD2 foci were scored. *, $P < 0.05$; **, $P < 0.01$; ***, $P < 0.001$, with comparison to untreated cells. (C) and (D), BJ-TERT cells were treated identically to that described for HeLa cells above. At least 300 nuclei were scored for each treatment and these experiments were performed three times with similar results. Error bars represent the standard errors of the means from three independent experiments.



examined [32]. In four out of five lines examined in this study, EPZ-6438 treatment led to an increase in levels of FANCD2 monoubiquitination. The mechanism(s) by which inhibition of PRC2/EZH2 and decreased global levels of H3K27me3 would lead to activation of the FA pathway remain to be clearly elucidated. Recent studies in the silkworm *Bombyx mori* have shown that PRC2-mediated H3K27me3 increases following exposure to UV irradiation [33]. One possibility is that, upon exposure to DNA damaging agents, transcription may need to be halted at loci that have incurred DNA damage. An inability to catalyze H3K27me3 and arrest transcription could lead to the formation of co-transcriptional RNA-DNA hybrids (R-loops). An important role for the FA proteins in the repair of R-loops has recently been established [34, 35]. However, our γ H2AX and RPA pS4/8 results strongly suggest a DNA damage-independent mode of action for BRD4770. An alternative hypothesis is that BRD4770 treatment - possibly *via* both G9a and PRC2/ EZH2 inhibition - leads to the general establishment of a transcriptionally permissive chromatin state, which leads to the recruitment of factors that promote homologous recombination (HR) DNA repair, such as FANCD2 and FANCI [13, 36]. Consistent with this hypothesis, Aymard *et al* have recently shown that HR factors are enriched at transcriptionally active chromatin [37]. It is important to note, however, that BRD4770-induced activation of the FA pathway most likely does not occur solely *via* the inhibition of PRC2/EZH2: BRD4770 induces FANCD2/I monoubiquitination more robustly than the EZH2-specific inhibitor EPZ-6438, and EPZ-6438 treatment results in more pronounced decreases in levels of H3K27me3. Therefore, other mechanisms are likely to contribute to the observed effects of BRD4770. In our study, we also detected

Figure 8: Inhibition of class I and II HDACs sensitizes cells to the cytotoxic effects of mitomycin C. BJ-TERT cells were exposed to the indicated concentrations of mitomycin C (MMC) in the absence or presence of (A) 5 mM sodium butyrate (NaB), (B) 331 nM trichostatin A (TSA), or (C) 10 mM nicotinamide (NAM) and cellular proliferation was determined using the CellTiter 96® AQ_{ueous} One Solution Cell Proliferation (MTS) assay. Error bars represent the standard errors of the means from three independent experiments.



increased phosphorylation of CHK1 S345 following BRD4770 exposure, indicating activation of the ATR-CHK1 checkpoint-signaling pathway. Numerous studies have indicated an important role for this pathway in signaling aberrant changes in chromatin structure [38–40]. One possibility is that BRD4770-induced changes in chromatin state lead to activation of ATR, phosphorylation of CHK1 and monoubiquitination of FANCD2, leading to activation of the intra-S-phase checkpoint. These findings are consistent with a large body of evidence linking the ATR-CHK1 signaling pathway to the activation of the FA pathway [41–44]. However, while BRD4770 treatment for 24 h did lead to an accumulation of cells in S-phase, exposure to BRD4770 for longer periods - when levels of phosphorylated CHK1 S345 and monoubiquitinated FANCD2 were maximal - did not appear to result in an overt S-phase arrest. Further experiments will be required to determine the relationship between changes in chromatin state, activation of the ATR-CHK1-FANCD2 axis and maintenance of the intra-S-phase checkpoint.

Here, we have also established that chemical inhibition of class I and II HDACs leads to attenuation of FANCD2 and FANCI monoubiquitination in BJ-TERT cells, with a less pronounced effect in HeLa cells, and significant reductions in FANCD2 nuclear foci formation in both HeLa and BJ-TERT cells. FANCD2/I monoubiquitination and nuclear foci are not strictly coupled: *Usp1*^{-/-} murine cells exhibit increased FANCD2 monoubiquitination in the absence of nuclear foci formation [45]. Thus, under the conditions examined, our findings point to an important role for histone deacetylation in facilitating the efficient activation of the FA pathway. Previous studies in the budding yeast *S. cerevisiae*, have shown that valproic acid (VPA), a class I and II HDACi,

inhibits Mec1 (orthologue of human ATR) signaling [46]. This is consistent with our observation of reduced ICL-inducible CHK1 S345 phosphorylation following HDAC inhibition with SAHA and TSA. Taken together with our BRD4770 findings, our results indicate that the ATR-CHK1 signaling pathway responds to changes in chromatin structure, and that phosphorylation and activation of CHK1 correlates with monoubiquitination and activation of FANCD2.

Several studies have established that, during the very early stages of DSB repair - seconds to minutes - a transient repressive chromatin state is first established, characterized by the spreading of HP1 and H3K9me_{2/3} [47]. The multisubunit NuRD repressor complex is rapidly recruited to sites of DNA damage where it promotes histone deacetylation and chromatin remodeling [48–50]. This may be necessary to restrict transcription in the immediate vicinity of the damaged site and to promote the recruitment of repair factors [47]. A failure to rapidly establish this transient repressive chromatin state would be predicted to lead to inefficient activation of DNA repair pathways, as we have observed following ICL treatment and HDAC inhibition. In contrast, a failure to catalyze H3K27me₃ upon exposure to BRD4770 or EPZ-6438 may lead to persistent, constitutively open/relaxed chromatin, which in turn may promote the inadvertent activation of repair mechanisms, as previously shown [51].

In summary, our results establish that chromatin state is an important determinant of the activation of the FA pathway. Our findings also suggest that combination chemotherapy comprising ICL-inducing agents and HDAC inhibitors may be an effective strategy for certain cancers. Recent studies have identified three functional modules within the FA core complex: the FANCB-FANCL-FAAP100 module, which provides the essential

monoubiquitination catalytic activity, and the FANCA-FANCG-FAAP20 and FANCC-FANCE-FANCF modules, which are thought to promote the recruitment of the core complex to chromatin [52, 53]. The majority of FA patients harbor mutations in the *FANCA* and *FANCG* genes, and FANCD2/I monoubiquitination is defective in >95% of FA patients [54]. Based on our findings, it is conceivable that the chromatin recruitment of the monoubiquitination catalytic module could be promoted *via* chemical modification of chromatin state, raising the prospect of epigenetics-based therapeutic approaches for certain FA complementation groups.

MATERIALS AND METHODS

Cell culture

The osteosarcoma cell line U2OS, the cervical carcinoma cell line HeLa, and the hTERT-immortalized BJ-TERT cells were grown in DMEM supplemented with 15% v/v fetal bovine serum, 2 mM L-glutamine, 50 U/mL penicillin, and 50 µg/mL streptomycin. HCT116 p53^{+/+} and p53^{-/-} cells were grown in McCoy's 5A medium containing the same supplements [55]. MCF10A mammary epithelial cells were grown in DMEM F12 supplemented with 5% v/v horse serum, 20 ng/ml epidermal growth factor, 0.5 mg/ml hydrocortisone, 100 ng/ml cholera toxin, 10 µg/ml insulin, 2 mM L-glutamine, 50 U/mL penicillin, and 50 µg/mL streptomycin.

Chemicals

The structures of all chemicals used in this study are shown in Supplementary Figure 5. The following chemicals were used: BRD4770 (histone methyltransferase inhibitor VI) (C₂₅H₂₃N₃O₃) (382194; EMD Millipore), BIX01294 (C₂₈H₃₈N₆O₂·3HCl·xH₂O) (B9311; Sigma), GSK-J1 (histone lysine demethylase inhibitor VII) (C₂₂H₂₃N₅O₂) (420204; EMD Millipore), PBIT (histone lysine demethylase inhibitor IX) (C₁₄H₁₁NOS) (505299; EMD Millipore), UNC0646 (C₃₆H₅₉N₇O₂) (SML0633; Sigma), BIX01338 (C₃₂H₂₄F₃N₃O₆·xH₂O) (B5313; Sigma), DZNep (3-Deazaneplanocin A) (C₁₂H₁₄N₄O₃) (13828; Cayman Chemical), EPZ-6438 (Tazemetostat) (C₃₄H₄₄N₄O₄) (S7128; Selleckchem), SAHA (Vorinostat) (C₁₄H₂₀N₂O₃) (SML0061; Sigma), Trichostatin A (TSA) (C₁₇H₂₂N₂O₃) (T1952; Sigma), Mitomycin C (MMC) (C₁₅H₁₈N₄O₅) (BP25312; Fisher Scientific), and Etoposide (VP-16) (C₂₉H₃₂O₁₃) (E1383; Sigma).

Immunoblotting and antibodies

For immunoblotting analysis, cell pellets were washed in PBS and lysed in 2% w/v SDS, 50 mM Tris-HCl, 10 mM EDTA. Proteins were resolved on NuPage 3-8% w/v Tris- Acetate or 4-12% w/v Bis-Tris gels (Invitrogen) and transferred to polyvinylidene difluoride (PVDF) membranes. The following antibodies were used: mouse monoclonal sera against γ H2AX (05-636; Millipore), HDAC1 (5356; Cell Signaling), HDAC2 (5113; Cell Signaling), HP1 α (05-689; Millipore), PCNA (sc-56; Santa Cruz Biotechnology), RPA (NA18; Calbiochem), and α -tubulin (MS-581-PO; Neomarkers), rabbit monoclonal serum against CHK1 pS345 (2348; Cell Signaling), and rabbit polyclonal sera against CHK2 pT68 (2661; Cell Signaling), EZH2 (5246S; Cell Signaling), FANCA (ABP6201; Cascade), FANCD2 (NB100-182; Novus Biologicals), FANCI (A301-254A; Bethyl Laboratories), H2A (07-146; Millipore), H3K27me3 (9733P; Cell Signaling), H4K16ac (07-329; Millipore), RPA pS4/8 (A300-245A; Bethyl), USP1 (a kind gift from Tony T. Huang, New York University), and UBE2T (A301-874A; Bethyl).

Immunofluorescence microscopy

For immunofluorescence microscopy (IF) analysis, cells were seeded in 4-well tissue culture slides (BD Falcon) in the presence or absence of drug(s) for 24 h. Soluble cellular proteins were pre-permeabilized with 0.3% v/v Triton X-100 and cells were fixed in 4% w/v paraformaldehyde and 2% w/v sucrose at 4°C followed by permeabilization in 0.3% v/v Triton X-100 in PBS. Fixed cells were blocked for 30 minutes in antibody dilution buffer (5% v/v goat serum, 0.1% v/v NP-40, in PBS) and

incubated with primary antibody for 1 h. Cells were washed three times in PBS, as well as permeabilization buffer, and incubated for 30 min at room temperature with an Alexa Fluor 488-conjugated secondary antibody and the slides were counterstained and mounted in vectashield plus 4',6-diamidino-2-phenylindole dihydrochloride (DAPI) (Vector Laboratories). Nuclear foci were scored using a Zeiss AxioImager.A1 upright epifluorescence microscope with AxioVision LE 4.6 image acquisition software. Primary antibodies used for IF were anti-FANCD2 (NB100-182; Novus Biologicals), anti-FANCI (A300-212A; Bethyl Laboratories), and anti- γ H2AX (05-636; Millipore). Statistical significance was determined using paired two-tailed Student's *t*-test analysis.

Chromatin fractionation

Cells were plated at density of 3×10^6 cells in 15 cm² dishes. The following day, cells were treated with 200 nM MMC for 24 h. Cells were harvested and resuspended in ice-cold PBS. A portion of the pellet was retained as a whole cell lysate (W). The remaining pellet was lysed on ice in cytoskeletal buffer (CSK) (300 mM Sucrose, 100 mM NaCl, 3 mM MgCl₂, 0.5% v/v Triton-X-100, 1 mM EGTA, 10 mM PIPES, pH 6.8). The supernatant, containing soluble cytoplasmic and nuclear proteins, was collected as the soluble fraction (S). The remaining pellet, containing chromatin-associated and nuclear insoluble proteins (C), and the whole-cell lysate pellet, were lysed in 2% SDS lysis buffer with sonication for 10 s at 10% amplitude using a Fisher Scientific Model 500 Ultrasonic Dismembrator.

Cell proliferation assay

Cells were plated at a density of 10,000 cells/well in 96-well dishes, incubated in the absence or presence of drug(s) for 48 h. CellTiter 96® AQ_{ueous} One Solution Reagent (MTS) (Promega) was added directly to the wells, incubated for a further 2 h, and the absorbance at 490 nm was measured using a 96-well Bio-Rad 680 microplate reader.

Cell-cycle analysis

Cells were plated at a density of 1×10^6 cells in 10 cm² dishes. The following day, cells were incubated in the absence or presence of 2, 5, and 10 μ M BRD4770 for 24, 48, and 72 h. Cells were resuspended in 0.1 mL PBS and fixed by adding 1 mL ice-cold methanol. Cells were washed in PBS and incubated in 50 μ g/mL propidium iodide (PI) (Sigma) and 30 U/mL RNase A for 10 min at 37°C, followed by analysis using a BD FACSVerser flow cytometer. The percentages of cells in G1, S, and G2/M were determined by analyzing PI histograms with FlowJo V10.2 software.

Authors' contributions

DAV performed the majority of the experiments and data analysis, and contributed to designing experiments and writing the manuscript. JLG assisted DAV with experiments. MAR performed the initial HMT and HDM experiments. MM performed the cell MAR performed the initial HMT and HDM experiments. MM performed the cell proliferation

assays. NGH conceived the study, analyzed the data, and wrote the manuscript.

ACKNOWLEDGMENTS

We thank members of the Howlett laboratory for critical reading of this manuscript and for helpful discussions. We also thank Dr. Adrian Bracken of the Smurfit Institute of Genetics at Trinity College Dublin for helpful advice on EZH2 reagents.

CONFLICTS OF INTEREST

The authors declare that they have no competing financial interests.

FUNDING

This work was supported by National Institutes of Health/National Heart, Lung and Blood Institute grant R01HL101977 (NGH); Rhode Island IDeA Network of Biomedical Research Excellence (RI-INBRE) grant P20GM103430 from the National Institute of General Medical Sciences; and Rhode Island Experimental Program to Stimulate Competitive Research (RI-EPSCoR) grant #1004057 from the National Science Foundation.

Abbreviations

HAT: histone acetyltransferase; HDAC: histone deacetylases; HDM: histone demethylase; HMT: histone methyltransferase; ICL: DNA interstrand crosslink; MMC: mitomycin C; NT: no treatment; VP-16: etoposide.

REFERENCES

1. Miller KM and Jackson SP. Histone marks: repairing DNA breaks within the context of chromatin. *Biochem Soc Trans.* 2012; 40:370-376.
2. Price BD and D'Andrea AD. Chromatin remodeling at DNA double-strand breaks. *Cell.* 2013; 152:1344-1354.
3. Soria G, Polo SE and Almouzni G. Prime, repair, restore: the active role of chromatin in the DNA damage response. *Mol Cell.* 2012; 46:722-734.
4. Huang H, Sabari BR, Garcia BA, Allis CD and Zhao Y. SnapShot: histone modifications. *Cell.* 2014; 159:458-458 e451.
5. Kusch T, Florens L, Macdonald WH, Swanson SK, Glaser RL, Yates JR, 3rd, Abmayr SM, Washburn MP and Workman JL. Acetylation by Tip60 is required for selective histone variant exchange at DNA lesions. *Science.* 2004; 306:2084-2087.
6. Miller KM, Tjeertes JV, Coates J, Legube G, Polo SE, Britton S and Jackson SP. Human HDAC1 and HDAC2 function in the DNA-damage response to promote DNA nonhomologous end-joining. *Nat Struct Mol Biol.* 2010; 17:1144-1151.
7. Murr R, Loizou JI, Yang YG, Cuenin C, Li H, Wang ZQ and Herceg Z. Histone acetylation by Trrap-Tip60 modulates loading of repair proteins and repair of DNA double-strand breaks. *Nat Cell Biol.* 2006; 8:91-99.
8. Kim H and D'Andrea AD. Regulation of DNA cross-link repair by the Fanconi anemia/BRCA pathway. *Genes Dev.* 2012; 26:1393-1408.
9. Schlacher K, Wu H and Jasin M. A distinct replication fork protection pathway connects Fanconi anemia tumor suppressors to RAD51-BRCA1/2. *Cancer Cell.* 2012; 22:106-116.

10. Moldovan GL and D'Andrea AD. How the Fanconi anemia pathway guards the genome. *Annu Rev Genet.* 2009; 43:223-249.
11. Walden H and Deans AJ. The Fanconi anemia DNA repair pathway: structural and functional insights into a complex disorder. *Annu Rev Biophys.* 2014; 43:257-278.
12. Garcia-Higuera I, Taniguchi T, Ganesan S, Meyn MS, Timmers C, Hejna J, Grompe M and D'Andrea AD. Interaction of the Fanconi anemia proteins and BRCA1 in a common pathway. *Mol Cell.* 2001; 7:249-262.
13. Sims AE, Spiteri E, Sims RJ, 3rd, Arita AG, Lach FP, Landers T, Wurm M, Freund M, Neveling K, Hanenberg H, Auerbach AD and Huang TT. FANCI is a second monoubiquitinated member of the Fanconi anemia pathway. *Nat Struct Mol Biol.* 2007; 14:564-567.
14. Smogorzewska A, Matsuoka S, Vinciguerra P, McDonald ER, 3rd, Hurov KE, Luo J, Ballif BA, Gygi SP, Hofmann K, D'Andrea AD and Elledge SJ. Identification of the FANCI protein, a monoubiquitinated FANCD2 paralog required for DNA repair. *Cell.* 2007; 129:289-301.
15. Kratz K, Schopf B, Kaden S, Sendoel A, Eberhard R, Lademann C, Cannavo E, Sartori AA, Hengartner MO and Jiricny J. Deficiency of FANCD2-associated nuclease KIAA1018/FAN1 sensitizes cells to interstrand crosslinking agents. *Cell.* 2010; 142:77-88.
16. MacKay C, Declais AC, Lundin C, Agostinho A, Deans AJ, MacArtney TJ, Hofmann K, Gartner A, West SC, Helleday T, Lilley DM and Rouse J. Identification of KIAA1018/ FAN1, a DNA repair nuclease recruited to DNA damage by monoubiquitinated FANCD2. *Cell.* 2010; 142:65-76.

17. Smogorzewska A, Desetty R, Saito TT, Schlabach M, Lach FP, Sowa ME, Clark AB, Kunkel TA, Harper JW, Colaiacovo MP and Elledge SJ. A genetic screen identifies FAN1, a Fanconi anemia-associated nuclease necessary for DNA interstrand crosslink repair. *Mol Cell*. 2010; 39:36-47.
18. Yamamoto KN, Kobayashi S, Tsuda M, Kurumizaka H, Takata M, Kono K, Jiricny J, Takeda S and Hirota K. Involvement of SLX4 in interstrand cross-link repair is regulated by the Fanconi anemia pathway. *Proc Natl Acad Sci U S A*. 2011; 108:6492-6496.
19. Yuan Y, Wang Q, Paulk J, Kubicek S, Kemp MM, Adams DJ, Shamji AF, Wagner BK and Schreiber SL. A small-molecule probe of the histone methyltransferase G9a induces cellular senescence in pancreatic adenocarcinoma. *ACS Chem Biol*. 2012; 7:1152-1157.
20. Greiner D, Bonaldi T, Eskeland R, Roemer E and Imhof A. Identification of a specific inhibitor of the histone methyltransferase SU(VAR)3-9. *Nat Chem Biol*. 2005; 1:143-145.
21. Kubicek S, O'Sullivan RJ, August EM, Hickey ER, Zhang Q, Teodoro ML, Rea S, Mechtler K, Kowalski JA, Homon CA, Kelly TA and Jenuwein T. Reversal of H3K9me2 by a small-molecule inhibitor for the G9a histone methyltransferase. *Mol Cell*. 2007; 25:473-481.
22. Montes de Oca R, Andreassen PR, Margossian SP, Gregory RC, Taniguchi T, Wang X, Houghtaling S, Grompe M and D'Andrea AD. Regulated interaction of the Fanconi anemia protein, FANCD2, with chromatin. *Blood*. 2005; 105:1003-1009.

23. Rogakou EP, Pilch DR, Orr AH, Ivanova VS and Bonner WM. DNA double-stranded breaks induce histone H2AX phosphorylation on serine 139. *J Biol Chem.* 1998; 273:5858-5868.
24. Vassin VM, Wold MS and Borowiec JA. Replication protein A (RPA) phosphorylation prevents RPA association with replication centers. *Mol Cell Biol.* 2004; 24:1930-1943.
25. Machida YJ, Machida Y, Chen Y, Gurtan AM, Kupfer GM, D'Andrea AD and Dutta A. UBE2T is the E2 in the Fanconi anemia pathway and undergoes negative autoregulation. *Mol Cell.* 2006; 23:589-596.
26. Laugesen A, Hojfeldt JW and Helin K. Role of the polycomb repressive complex 2 (PRC2) in transcriptional regulation and cancer. *Cold Spring Harb Perspect Med.* 2016; 6.
27. Tan J, Yang X, Zhuang L, Jiang X, Chen W, Lee PL, Karuturi RK, Tan PB, Liu ET and Yu Q. Pharmacologic disruption of Polycomb-repressive complex 2-mediated gene repression selectively induces apoptosis in cancer cells. *Genes Dev.* 2007; 21:1050-1063.
28. Liu F, Barsyte-Lovejoy D, Allali-Hassani A, He Y, Herold JM, Chen X, Yates CM, Frye SV, Brown PJ, Huang J, Vedadi M, Arrowsmith CH and Jin J. Optimization of cellular activity of G9a inhibitors 7-aminoalkoxy-quinazolines. *J Med Chem.* 2011; 54:6139-6150.
29. Knutson SK, Kawano S, Minoshima Y, Warholc NM, Huang KC, Xiao Y, Kadowaki T, Uesugi M, Kuznetsov G, Kumar N, Wigle TJ, Klaus CR, Allain CJ, et al.

Selective inhibition of EZH2 by EPZ-6438 leads to potent antitumor activity in EZH2-mutant non-Hodgkin lymphoma. *Mol Cancer Ther.* 2014; 13:842-854.

30. Knutson SK, Wigle TJ, Warholic NM, Sneeringer CJ, Allain CJ, Klaus CR, Sacks JD, Raimondi A, Majer CR, Song J, Scott MP, Jin L, Smith JJ, et al. A selective inhibitor of EZH2 blocks H3K27 methylation and kills mutant lymphoma cells. *Nat Chem Biol.* 2012; 8:890-896.

31. Miranda TB, Cortez CC, Yoo CB, Liang G, Abe M, Kelly TK, Marquez VE and Jones PA. DZNep is a global histone methylation inhibitor that reactivates developmental genes not silenced by DNA methylation. *Mol Cancer Ther.* 2009; 8:1579-1588.

32. Knutson SK, Warholic NM, Wigle TJ, Klaus CR, Allain CJ, Raimondi A, Porter Scott M, Chesworth R, Moyer MP, Copeland RA, Richon VM, Pollock RM, Kuntz KW, et al. Durable tumor regression in genetically altered malignant rhabdoid tumors by inhibition of methyltransferase EZH2. *Proc Natl Acad Sci U S A.* 2013; 110:7922-7927.

33. Li Z, Mon H, Mitsunobu H, Zhu L, Xu J, Lee JM and Kusakabe T. Dynamics of polycomb proteins-mediated histone modifications during UV irradiation-induced DNA damage. *Insect Biochem Mol Biol.* 2014; 55:9-18.

34. Garcia-Rubio ML, Perez-Calero C, Barroso SI, Tumini E, Herrera-Moyano E, Rosado IV and Aguilera A. The Fanconi anemia pathway protects genome integrity from R-loops. *PLoS Genet.* 2015; 11:e1005674.

35. Schwab RA, Nieminuszczy J, Shah F, Langton J, Lopez Martinez D, Liang CC, Cohn MA, Gibbons RJ, Deans AJ and Niedzwiedz W. The Fanconi anemia pathway

maintains genome stability by coordinating replication and transcription. *Mol Cell*. 2015; 60:351-361.

36. Nakanishi K, Cavallo F, Perrouault L, Giovannangeli C, Moynahan ME, Barchi M, Brunet E and Jasin M. Homology-directed Fanconi anemia pathway cross-link repair is dependent on DNA replication. *Nat Struct Mol Biol*. 2011; 18:500-503.

37. Aymard F, Bugler B, Schmidt CK, Guillou E, Caron P, Briois S, Iacovoni JS, Daburon V, Miller KM, Jackson SP and Legube G. Transcriptionally active chromatin recruits homologous recombination at DNA double-strand breaks. *Nat Struct Mol Biol*. 2014; 21:366-374.

38. Hoek M and Stillman B. Chromatin assembly factor 1 is essential and couples chromatin assembly to DNA replication in vivo. *Proc Natl Acad Sci U S A*. 2003; 100:12183-12188.

39. Smith-Roe SL, Nakamura J, Holley D, Chastain PD, 2nd, Rosson GB, Simpson DA, Ridpath JR, Kaufman DG, Kaufmann WK and Bultman SJ. SWI/SNF complexes are required for full activation of the DNA-damage response. *Oncotarget*. 2015; 6:732-745.

40. Vassileva I, Yanakieva I, Peycheva M, Gospodinov A and Anachkova B. The mammalian INO80 chromatin remodeling complex is required for replication stress recovery. *Nucleic Acids Res*. 2014; 42:9074-9086.

41. Andreassen PR, D'Andrea AD and Taniguchi T. ATR couples FANCD2 monoubiquitination to the DNA-damage response. *Genes Dev*. 2004; 18:1958-1963.

42. Guervilly JH, Mace-Aime G and Rosselli F. Loss of CHK1 function impedes DNA damage-induced FANCD2 monoubiquitination but normalizes the abnormal G2 arrest in Fanconi anemia. *Hum Mol Genet.* 2008; 17:679-689.
43. Ho GP, Margossian S, Taniguchi T and D'Andrea AD. Phosphorylation of FANCD2 on two novel sites is required for mitomycin C resistance. *Mol Cell Biol.* 2006; 26:7005-7015.
44. Pichierri P and Rosselli F. The DNA crosslink-induced S-phase checkpoint depends on ATR-CHK1 and ATR-NBS1-FANCD2 pathways. *EMBO J.* 2004; 23:1178-1187.
45. Kim JM, Parmar K, Huang M, Weinstock DM, Ruit CA, Kutok JL and D'Andrea AD. Inactivation of murine *Usp1* results in genomic instability and a Fanconi anemia phenotype. *Dev Cell.* 2009; 16:314-320.
46. Robert T, Vanoli F, Chiolo I, Shubassi G, Bernstein KA, Rothstein R, Botrugno OA, Parazzoli D, Oldani A, Minucci S and Foiani M. HDACs link the DNA damage response, processing of double-strand breaks and autophagy. *Nature.* 2011; 471:74-79.
47. Gursoy-Yuzugullu O, House N and Price BD. Patching Broken DNA: Nucleosome Dynamics and the Repair of DNA Breaks. *J Mol Biol.* 2016; 428:1846-1860.
48. Ayrapetov MK, Gursoy-Yuzugullu O, Xu C, Xu Y and Price BD. DNA double-strand breaks promote methylation of histone H3 on lysine 9 and transient formation of repressive chromatin. *Proc Natl Acad Sci U S A.* 2014; 111:9169-9174.
49. Chou DM, Adamson B, Dephore NE, Tan X, Nottke AC, Hurov KE, Gygi SP, Colaiacovo MP and Elledge SJ. A chromatin localization screen reveals poly (ADP

ribose)- regulated recruitment of the repressive polycomb and NuRD complexes to sites of DNA damage. *Proc Natl Acad Sci U S A*. 2010; 107:18475-18480.

50. Smeenk G, Wiegant WW, Vrolijk H, Solari AP, Pastink A and van Attikum H. The NuRD chromatin-remodeling complex regulates signaling and repair of DNA damage. *J Cell Biol*. 2010; 190:741-749.

51. Bakkenist CJ and Kastan MB. DNA damage activates ATM through intermolecular autophosphorylation and dimer dissociation. *Nature*. 2003; 421:499-506.

52. Huang Y, Leung JW, Lowery M, Matsushita N, Wang Y, Shen X, Huong D, Takata M, Chen J and Li L. Modularized functions of the Fanconi anemia core complex. *Cell Rep*. 2014; 7:1849-1857.

53. Rajendra E, Oestergaard VH, Langevin F, Wang M, Dornan GL, Patel KJ and Passmore LA. The genetic and biochemical basis of FANCD2 monoubiquitination. *Mol Cell*. 2014; 54:858-869.

54. FARF I. (2014). *Fanconi Anemia: Guidelines for Diagnosis and Management*. (Eugene, OR: Fanconi Anemia Research Fund, Inc).

55. Bunz F, Dutriaux A, Lengauer C, Waldman T, Zhou S, Brown JP, Sedivy JM, Kinzler KW and Vogelstein B. Requirement for p53 and p21 to sustain G2 arrest after DNA damage. *Science*. 1998; 282:1497-1501.

Manuscript II

Unpublished works

Phosphorylation of FANCD2 regulates its function in a DNA damage independent manner

David A Vierra¹, Rebecca Boisvert², Advaita Madireddy³, Andrew Deans⁴ Carl Scildkraut³, Niall Howlett¹

¹ Department of Cell and Molecular Biology, University of Rhode Island, Kingston, Rhode Island, U.S.A

² Department of Cancer Biology, MD Anderson, Houston, Texas, U.S.A

³ Department of Cell Biology, Albert Einstein College of Medicine, Bronx, New York, U.S.A

⁴ Genome stability Unit, University of Melbourne, Parkville VIC 3010, Australia

Abstract

Fanconi anemia (FA) is a rare genetic disease characterized by early onset bone marrow failure, congenital defects and increased cancer susceptibility. FA is caused by mutation in any one of twenty two different genes. The main function of the proteins encoded by these genes is to resolve interstrand crosslinks (ICL) within DNA. ICLs present direct physical blocks to DNA replication. Upon induction of an ICL, a core complex of proteins will come together to create a multi-subunit ubiquitin ligase, catalyzes the monoubiquitination of FANCD2 and FANCI, thereby activating these two proteins and initiating ICL repair. In addition to monoubiquitination, FANCD2 and FANCI are known to be phosphorylated. To date, all known phospho-sites on FANCD2 and FANCI are phosphorylated only in the presence of DNA damage. These sites have been well characterized and their respective kinases have been identified. Our lab has found a novel phospho-cluster on FANCD2. This cluster is phosphorylated in a DNA damage independent fashion. The phosphorylation appears to be cell cycle specific, being at its peak in S phase. We have identified three candidate residues, proximal to K561, that may be the site of this phosphorylation. There is strong evidence that the kinase responsible for this phosphorylation is a cyclin dependent kinase (CDK). Phosphorylation at these sites abrogates FANCD2 monoubiquitination while dephosphorylation promotes monoubiquitination. Our data suggests that this phosphorylation may be acting as a “molecular switch” to activate FANCD2s function during DNA replication.

Introduction

Fanconi anemia (FA) is a rare, X-linked and autosomal recessive genetic disorder. Patients suffer from congenital abnormalities, pediatric bone marrow failure and cancer susceptibility. FA is caused by a biallelic mutation in any one of twenty two different genes (*FANCA*, *-B*, *-C*, *-D1/BRCA2*, *-D2*, *-E*, *-F*, *-G*, *-I*, *-J/BRIP1*, *-L*, *-M*, *-N/PALB2*, *-P/SLX4*, *O/RAD51C*, *Q/ERCC4*, *R/RAD51*, *S/BRCA1*, *T/UBE2T*, *-U/XRCC4*, *-V/REV7*, *-W/RFWD3*)[1-5]. These proteins function cooperatively in the FA-BRCA pathway to resolve interstrand crosslinks (ICL) within DNA. ICLs present direct physical blocks to DNA synthesis and are a cause of chromosomal instability. Upon the induction of an ICL a core complex of proteins, *FANCA/B/C/E/F/G/L/T* come together to form a multisubunit ubiquitin ligase. With the help of *FANCM*, *FAAP100/24/20* and *MHF1/2*, the core complex will be recruited to the ICL and promote the monoubiquitination of *FANCD2* and *FANCI*[3, 6, 7]. The monoubiquitination of *FANCD2* and *FANCI* is a key activating step in the pathway; a step is absent in over 90% of FA patients. Upon its monoubiquitination *FANCD2* and *FANCI* will work to recruit downstream proteins that will resolve the ICL in a homologous recombination (HR) mediated process[6, 8-10]. Without the FA pathway the ICL will be resolved in an error prone process known as non-homologous end joining (NHEJ), resulting in extensive DNA damage[11, 12].

In addition to monoubiquitination, *FANCD2* and *FANCI* are also post translationally modified (PTM) through phosphorylation. It has been shown that *FANCD2* is phosphorylated by ATM (Ataxia-telangiectasia mutated) in response to ionizing

radiation (IR). FANCD2 is also phosphorylated by ATR (ATM and Rad3-related) when cells are treated with ICL inducing agents[13-15]. It is thought that DNA damage dependent FANCD2 phosphorylation is key for its monoubiquitination and heterodimerization with FANCI. ATM/ATR are also responsible for FANCI phosphorylation. FANCI is phosphorylated in a DNA damage dependent manner on six SQ/TQ residues that are proximal to its site of monoubiquitination [16]. The phosphorylation of FANCI has been shown to function both upstream and downstream of monoubiquitination [17, 18].

Though the main function of FANCD2 is in the DNA damage response (DDR), there is evidence to show that it functions in other cellular processes. For example, FANCD2 is critical in the resolution of RNA:DNA hybrids known as R-loops [19]. There is also mounting evidence that suggests FANCD2 is involved in replication fork firing and stability[20-22]. The recent Molecular Cell paper by Madireddy *et al.* showed that FANCD2 is required for stability at common fragile sites (CFS) and that it may regulate dormant origin firing under replication stress[23]. In addition to this, FANCD2 has been shown to protect stalled replication forks from MRE11 degradation and, *via* its interaction with CtBP-interacting protein (CtIP), it is involved in replication fork restart[24, 25].

In this manuscript, I will present data that shows that FANCD2 is phosphorylated in a DNA damage independent cell cycle dependent manner. This phosphorylation is at its height during unperturbed S-phase of the cell cycle. Both *in-silico* and ex-vivo studies done by our lab suggest that a cyclin dependent kinase (CDK) is responsible for this phosphorylation. CDKs, along with their cyclin binding partners, are responsible for

regulation of the cell cycle, halting it if damage is present[26]. There is precedent for CDKs acting in the DDR, CDKs have been shown to phosphorylate BRCA1 and BRCA2 (both of which are within the FA-BRCA pathway)[27-29]. We have identified 3 putative CDK sites that are proximal to the sites of monoubiquitination. Two mutants have been created at these sites. One mutant cannot be phosphorylated (phospho-dead) and the other mutant behaves as if it is constitutively phosphorylated, (a phospho-mimetic). Surprisingly, it appears that the phospho-dead mutant is constitutively monoubiquitinated while the phospho-mimetic is deficient in monoubiquitination. This is at odds with the characterization of FANCI phosphorylation, in which phosphorylation promotes monoubiquitination [16, 18]. Our data also suggests that phosphorylation of FANCD2 may act as a “molecular switch” to activate other functions, in particular its roles in DNA replication. Characterization of these phosphorylation sites will shed light on the interplay between monoubiquitination and phosphorylation, highlighting new roles for FANCD2 and the importance of temporal regulation of monoubiquitination.

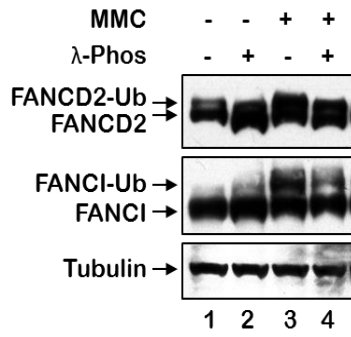
Results

Phosphorylation of FANCD2 is DNA damage independent and cell cycle dependent

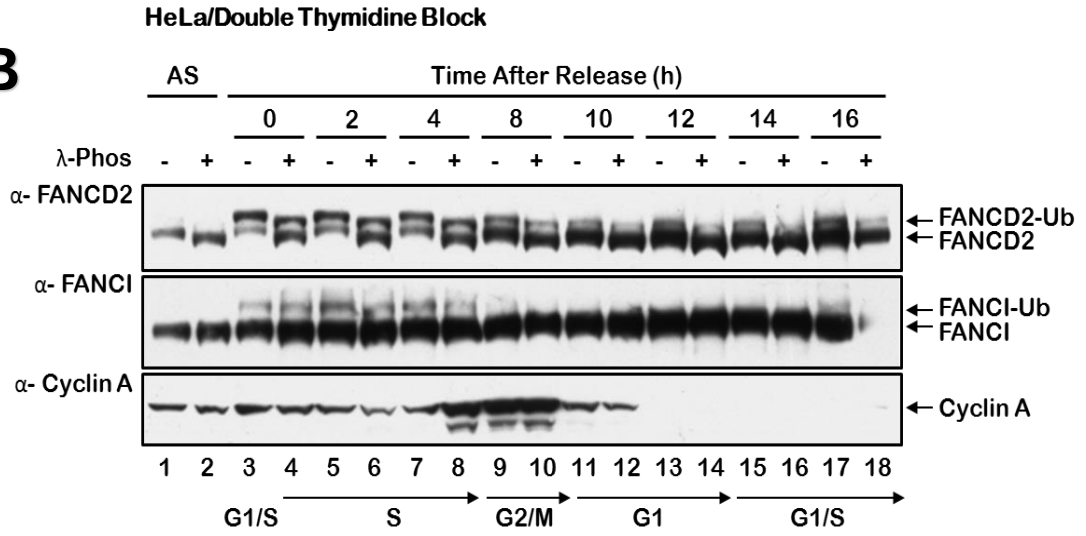
To elucidate whether FANCD2 phosphorylation was occurring in a DNA damage independent manner a simple experiment was performed. U2OS cells were treated

Figure 1. FANCD2 is monoubiquitinated in a DNA damage independent cell cycle dependent manner (A) U2OS cells were treated in the presence (+) or absence (-) of 200nM MMC. The pellet was split in half, one half was treated for 2 hours with lambda phosphatase (+) and the other was treated with phosphatase inhibitors (-). Blots were probed with against FANCD2, FANCI and alpha-tubulin (B) HeLa cells were blocked into late G1/S using a double thymidine block. The cells were released and time points were taken every 2 hours for 16 hours. The pellet was then split in half and treated with (+) and without (-) lambda phosphatase for 2 hours and immunoblotted against FANCD2, FANCI, and Cyclin A. AS, asynchronous whole-cell lysate

A



B

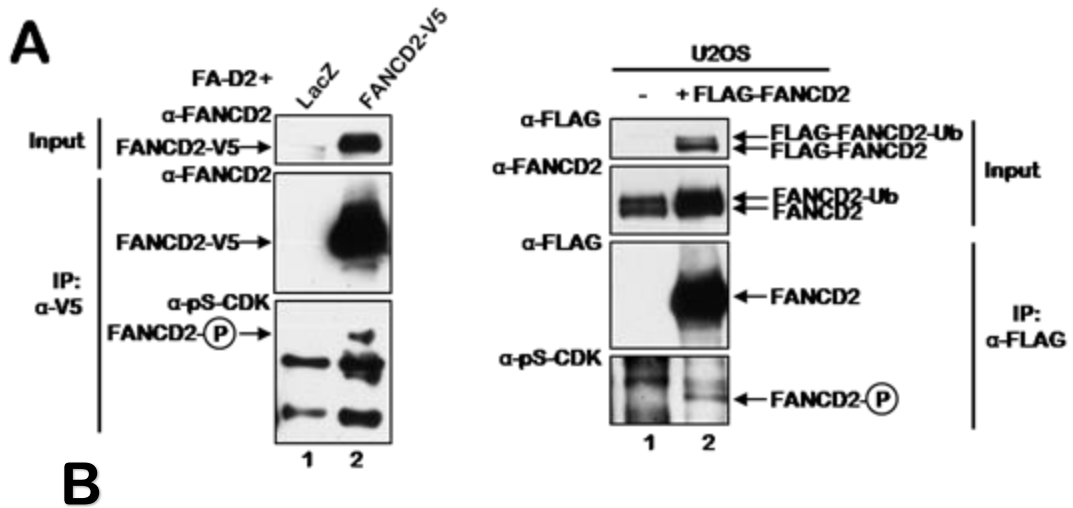


with and without the interstrand crosslinking agent mitomycin C (MMC). The lysates were then split in half, half were treated with phosphatase inhibitors and the other half were treated with lambda phosphatase. Lambda phosphatase cleaves phosphates off of serine, threonine and tyrosine residues. We observed a prominent mobility shift between our samples with and without lambda phosphatase. As is seen in lanes 1 and 2 of Figure 1A, this shift occurred in the absence of any DNA damage. Of note, there was not a similar shift in FANCI, signifying that FANCI is not as extensively phosphorylated as FANCD2. To pinpoint where in the cell cycle phosphorylation is occurring, HeLa cells were used to perform a double thymidine block, synchronizing cells in G1/S phase of the cell cycle. The cells were then released and time points were taken every two hours for 16 hours. A mobility shift between our untreated and lambda phosphatase treated samples was observed within S-phase. This signifies the hyper-phosphorylation of FANCD2 in S-phase (Figure 1B). The cell cycle checkpoint protein Cyclin A was used as a control for cell cycle progression, with its highest expression in late S early G2 of the cell cycle. Two important observations can be made from this experiment. 1) FANCD2 is extensively phosphorylated in the absence of DNA damage 2) This phosphorylation occurs to the largest degree during S-phase of the cell cycle.

FANCD2 phosphorylation is mediated by a cyclin dependent kinase

DNA damage independent phosphorylation of FANCD2 appears to be related to the cell cycle. With this in mind, we began to look for candidate kinases that could be performing this phosphorylation. Since we know the phosphorylation is cell cycle specific, we started investigating cell cycle specific kinases. This led us to CDKs, CDKs are active during S-

Figure 2. FANCD2 is a potential substrate of CDK phosphorylation. (A) FA-D2 cells stably expressing LacZ-V5 and FANCD2-V5 were immunoprecipitated with anti-V5 agarose and immune complexes were immunoblotted with anti-FANCD2 and anti-pSCDK. (B) U2OS and U2OS cells stably expressing 3X FLAG FANCD2-WT were immunoprecipitated with anti-FLAG agarose and immune complexes were immunoblotted with anti-FANCD2, anti-FLAG, and anti-pSCDK. (C) U2OS 3X FLAG FANCD2 immunoprecipitated as shown in (B), was used for phospho enrichment and further mass spectrometry analysis revealed several phosphorylated FANCD2 isoforms. *X.laevis* extract FANCD2 was pulled down in a similar fashion to (A) and underwent mass spectrometry analysis.



Species	Site	Peptide length
H. sapiens	S592	11
X. laevis	S726	12

phase of the cell cycle and, as previously stated, there is also precedence for CDKs phosphorylating DDR proteins. Moreover, some of these proteins are in the FA-BRCA pathway (BRCA1 and BRCA2) [26]. Two immunoprecipitations (IP) were performed to determine if FANCD2 is a CDK substrate. The first was performed in an FA-D2 cell line, cells lacking FANCD2, that stably express a FANCD2 construct with a C-terminal V5 tag (FANCD2-V5). A vector containing V5 tagged LacZ was used as a control. FANCD2-V5 was immunoprecipitated using V5-agarose. The second was performed in U2OS cells, transformed osteosarcoma cells, stably expressing 3xFLAG FANCD2 (FLAG-FANCD2). An IP was performed using FLAG agarose. In both IPs, the pull down product was probed with an antibody that recognizes serine residues phosphorylated by CDKs. The antibody detected a FANCD2 band in both IPs (Figure 2A), suggesting that FANCD2 is a CDK phosphorylation target. Mass spectrometry analysis of the U2OS 3xFLAG FANCD2 IP showed a phosphorylation of FANCD2 at S692. In addition, our collaborator at the University of Melbourne performed a similar experiment using *X. laevis* FANCD2 and found a phosphorylation at S726 following mass spectrometry analysis (Figure 2B). These both represent novel sites of phosphorylation.

FANCD2 contains a putative CDK cluster proximal to the site of monoubiquitination

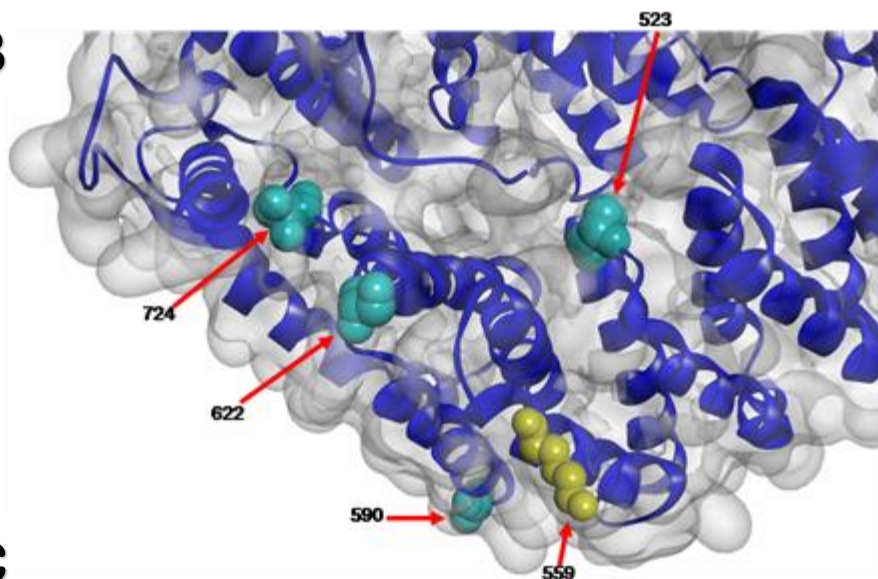
The CDK consensus sequence is [S/T*]PX[K/R][30], however, there are examples of proteins be phosphorylated by a CDK that only contain the S/P of the consensus sequence, such as BRCA1[31]. When the FANCD2 amino acid sequence was analyzed

Figure 3. FANCD2 contains a conserved putative CDK consensus site cluster. (A). A Clustal Omega multiple sequence alignment of three putative CDK phosphorylation sites, S525, S624, S726, in FANCD2 demonstrates strong evolutionary conservation. (B) Region of the mouse Fancd2 crystal structure represented as both surface and ribbons with S/P CDK consensus (teal) and the monoubiquitination site (yellow) indicated, using the program Discovery Studio. (C) FA-D2 cells stably expressing empty, FANCD2-WT,-TA, and -TD were incubated in the absence (-) and presence (+) of 250 nM MMC for 18 h, and whole-cell lysates were immunoblotted with antibodies to FANCD2, V5, FANCI and α -tubulin. The FANCD2-V5 and FANCI L/S ratios are the ratios of monoubiquitinated to nonubiquitinated protein, and were calculated by measuring protein band intensities using ImageJ image processing and analysis software (<http://rsb.info.nih.gov/ij/>).

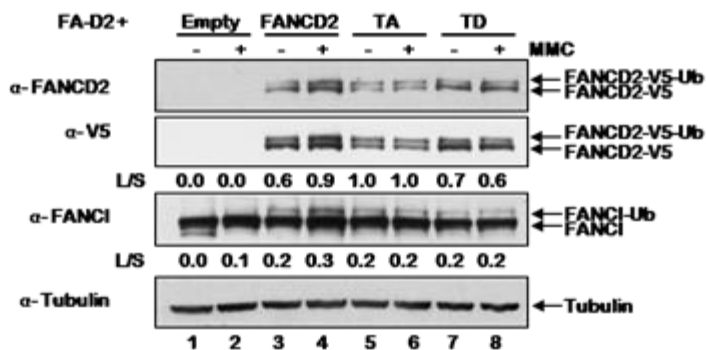
A

	S525		S624		S726	
<i>J. sapiens</i>	522	DNVSPQQI	621	SEQSPQAS	723	KVSPPLCL
<i>P. troglodytes</i>	394	DNVSPQQI	533	TEHSPWAS	646	KVSPPLCL
<i>M. musculus</i>	520	ENVSPQQI	620	TEHSPWAS	721	SVSSPLCL
<i>C. familiaris</i>	522	DNVSPQQI	619	SEQSPQAS	720	KVSPPLCL
<i>G. gallus</i>	525	QKIDECQI	622	CEQTEPEVL	725	RVSPPLCL
<i>X. tropicalis</i>	529	DNVNAQQI	626	SEQVPPAS	726	RVSPPLCL
<i>D. rerio</i>	523	DNVLSQQI	619	SESSPEPA	721	RVSPPLCL
<i>D. melanogaster</i>	555	SDLSLTCT	661	IGVSTESL	763	ACDSIYVL
<i>C. elegans</i>	369	HKLSIPPI	354	VKSSSALR	525	-SARLIE

B

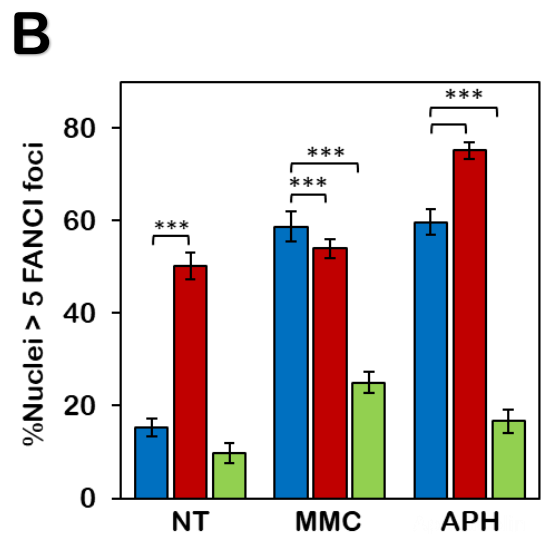
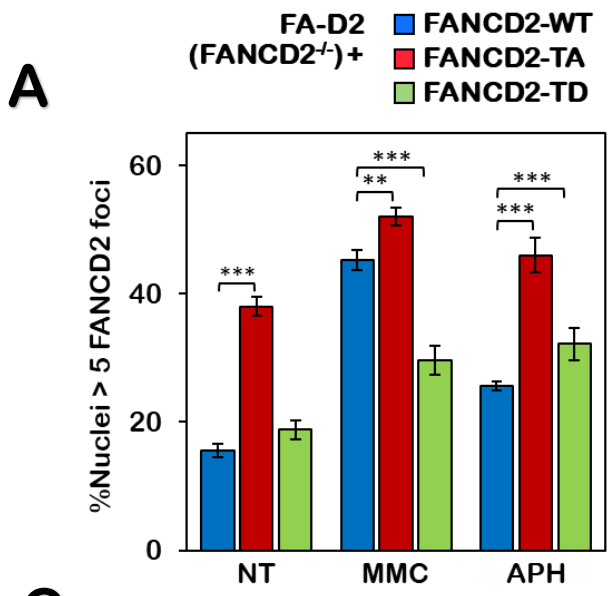


C

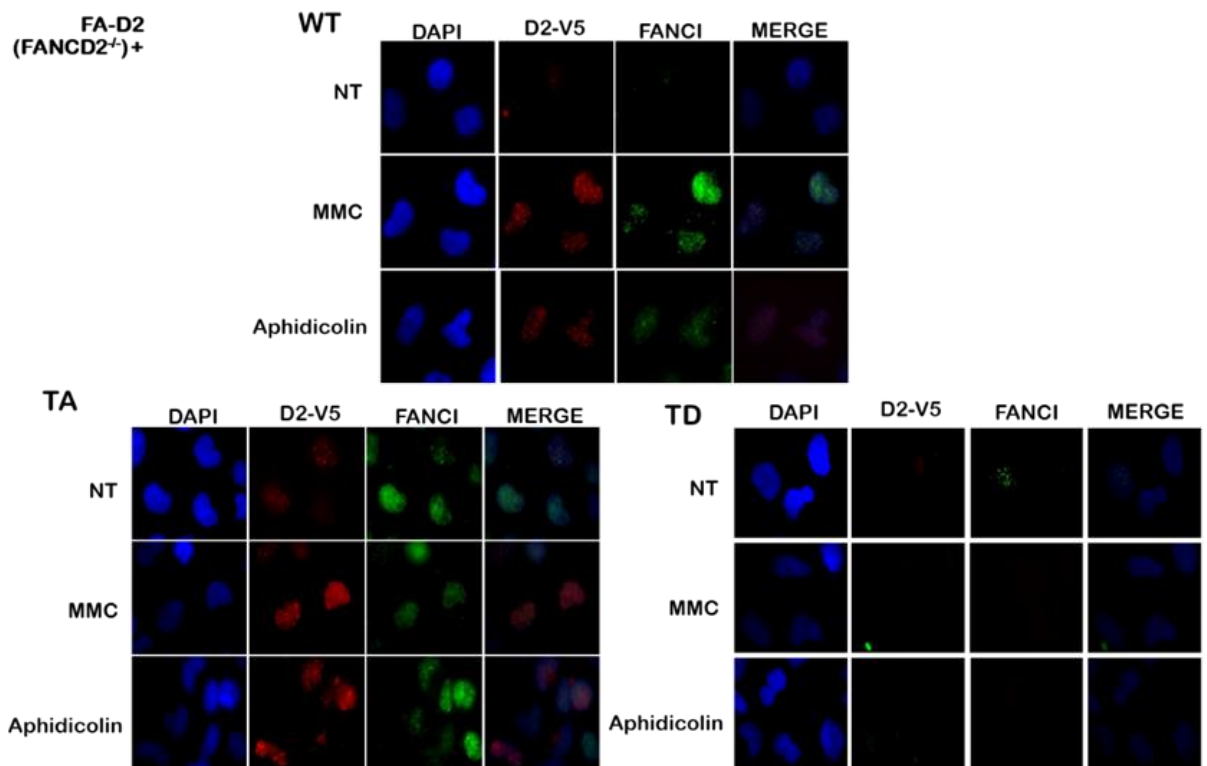


many putative CDK S/P sites were found (data not shown). To hone in on sites that might have an effect on DNA repair, *in-silico* analysis was performed. When the sites are mapped onto the mouse ID2 heterodimer (PDB ID:3S4W), human ID2 has yet to be crystallized, we see that four of these sites are proximal to K562, the site monoubiquitination in mouse *fancd2* (Figure 3B). In addition, when a multi-species alignment is performed using Clustal Omega three of these sites, S525, S264 and S726, demonstrate strong evolutionary conservation. The fourth site was on an uncrystallized loop within mouse *fancd2*, we did not recognize this site until much later so analysis of this site is ongoing. We hypothesized, based on their proximity to K561, that the three identified sites were the most likely to have an effect on FANCD2 monoubiquitination, based on their proximity to K561. Additionally, two of these sites, S592 and S724, were found in the mass spectrometry results discussed earlier. We next stably expressed two different V5-tagged FANCD2 mutants in a FA-D2 patient cell line. One mutant has S525, S264 and S726 mutated to alanines (TA), this mutant is unable to be phosphorylated at these sites. The second mutant has the same serines mutated to aspartic acids (TD), the negative charge on the aspartic acid acts as phospho-mimetic (FANCD2 appears constitutively phosphorylated at these sites). V5 tagged wildtype (WT) FANCD2 and an empty vector were stably expressed as controls. An experiment was performed in which each cell line was incubated with and without MMC. When we immunoblotted, probing for FANCD2-V5, we found that the TA mutant appeared to be constitutively monoubiquitinated while the TD mutant was deficient in monoubiquitination (Figure 3C).

Figure 4. Mutation of the FANCD2 CDK cluster alters both FANCD2 and FANCI foci formation (A) FA-D2 cells + WT-V5, TA-V5 or TD-V5 were treated with and without 200 nM MMC or 0.8 μ M APH. Cells were fixed and stained with a mouse polyclonal anti-V5 antibody and counterstained with DAPI. At least 300 nuclei were scored per treatment (B) FA-D2 cells + WT-V5, TA-V5 or TD-V5 were treated with and without 200nM MMC or .8 μ M APH. Cells were fixed and stained with a rabbit polyclonal anti-FANCI antibody and counterstained with DAPI. At least 300 nuclei were scored per treatment (C) Representative images of foci images. DAPI is in blue, FANCD2-V5 is in red and FANCI is in green. The merge is all three images overlaid



C



Phosphorylation of FANCD2 plays an important role in foci formation

There is evidence to suggest that monoubiquitination of FANCD2 and aggregation within the nucleus to form foci can be uncoupled, as seen in USP1 autocleavage mutants [32]. To examine if this was occurring in our mutants, cells were treated with both MMC and aphidicolin (APH), a known polymerase inhibitor and replication stressor[33]. The cells were fixed and stained for FANCD2-V5, FANCI and DAPI. The TA mutants had statistically significantly higher FANCD2-V5 and FANCI foci in the no treatment condition than either WT or TD (Figure 4A, B). Upon treatment with both MMC and APH, the TD mutant had statistically significant lower foci formation than either TA or WT. This indicates that not only is the TA mutant deficient in monoubiquitination but FANCD2 is unable to localize to the sites of damage within the nucleus. In addition, the TA mutant seems to be constitutively monoubiquitinated and form foci even in the absence of damage. It is noteworthy that the effects on foci formation also occurred in FANCI, indicating that phosphorylation of FANCD2 does not increase the monoubiquitination of FANCI but does increase its foci formation. This brings up questions about the importance of FANCD2 phosphorylation on FANCI-FANCD2 dimerization and aggregation within the nucleus.

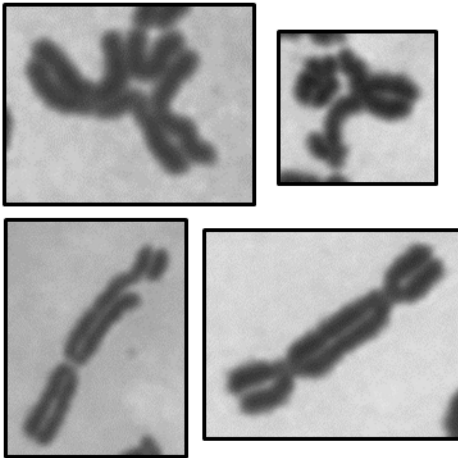
FANCD2 phosphorylation effects chromosomal stability

One of the hallmarks of Fanconi Anemia is hypersensitivity to DNA damaging agents. Chromosomal breakage analysis of peripheral blood samples treated with damaging

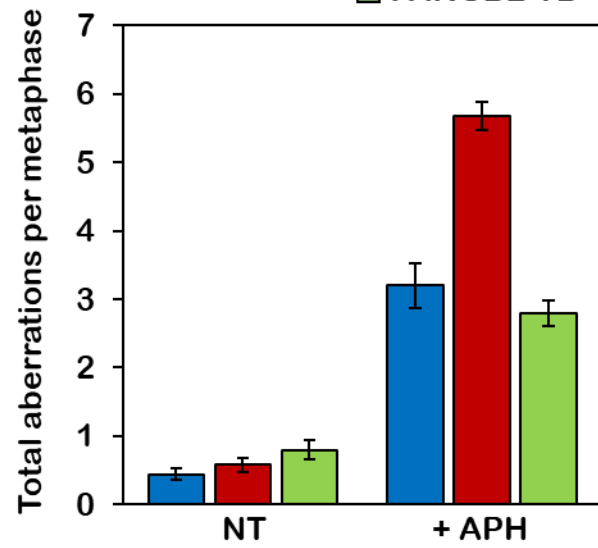
Figure 5. The phospho-dead TA mutant has a high concentration of chromosomal aberrations (A) Representative images of the types of chromosome aberrations - including radial formations, telomere fusions, dicentrics, and complex aberrations - observed in the TA mutant cells following .4 μ M APH treatment(B) FA-D2 cells + WT-V5, TA-V5 or TD-V5 were treated with and without .4 μ M APH for 24 hours, fixed and dropped onto slides and stained with giemsa. The slides were analyzed, counting aberration such as radial formations, telomere fusions, dicentrics, and complex aberrations. This is preliminary data; 50 metaphases were scored per condition

A

FA-D2
(FANCD2^{-/-}) +
FANCD2-TA

**B**

FA-D2 (FANCD2^{-/-}) +
■ FANCD2-WT (blue)
■ FANCD2-TA (red)
■ FANCD2-TD (green)



agents are often used in clinical setting to diagnose FA[34]. We performed metaphase spread analysis using our mutants, looking for chromosome gaps and breaks, dicentric chromosome and more complex chromosome aberrations such as radials. When our mutants were treated with low doses of APH, the TA mutant had a substantial increase in damage over both the WT and TD. The TD had slightly lower amounts of damage than the WT (Figure 6). Even though the TA mutant had both an increase in monoubiquitination and foci formation, this did not correlate to decreased chromosomal aberrations and the inverse seems to be true for the TD. We believe that this showcases the importance of controlling the timing of FANCD2 monoubiquitination. It is detrimental to chromosomal stability for FANCD2 to be constantly activated, FANCD2 monoubiquitination must be precisely timed in order for proper DNA repair to take place.

Mutation of the FANCD2 CDK cluster impacts fork restart following damage

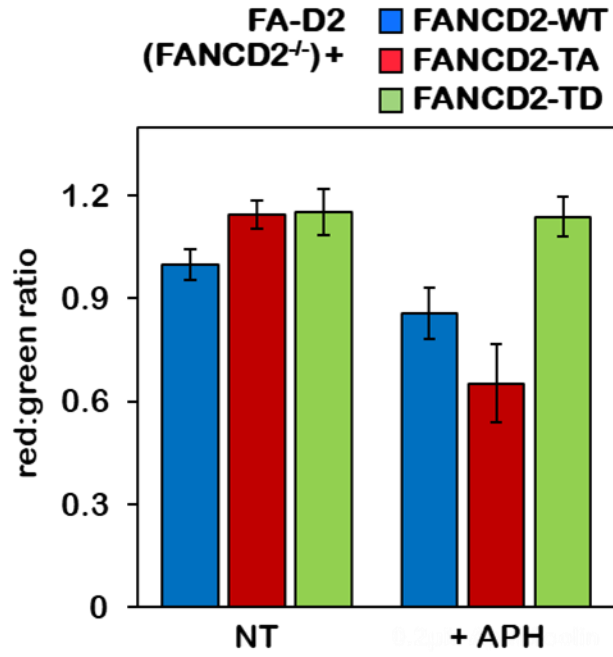
Our research has shown that FANCD2 is phosphorylated in S phase of the cell cycle and that this phosphorylation occurs in the absence of any DNA damage. These are interesting observations but they do not answer the basic question of what the purpose of this phosphorylation is. Since this phosphorylation is specific to S-phase, the logical inference is that the phosphorylation at these sites is somehow regulating FANCD2's function in DNA synthesis. To explore this, DNA strand analysis was performed to analyze both fork restart following damage and the affects our mutations have on the total DNA synthesis occurring. Cells were treated with 0.2 μ M APH for 12 hours, pulsed for 20 minutes with iodouridine followed by a 20 minute pulse with chlorouridine, these were stained red and green respectively. In addition, a single strand antibody was used that stains the total DNA

content of the cell. When these images are overlaid with the red/green images the percent of active replication can be calculated (Figure S4). When analyzing the red and green staining, we took the ratio of the red to the green. The length of the red portion represents fork progression directly after DNA damage, while the green portion has fully recovered and represents unperturbed synthesis. Without APH treatment there is a red:green ratio of around 1, which should be expected since there is nothing to hinder the replication fork (Figure 7A). APH treatment results in lower red:green ratios because the cells have to recover from the treatment before progressing, however the TA mutant has a lower red:green than either WT or TD (Figure 7A). This illustrates replication deficiencies in the TA mutant, in particular where fork restart is concerned.

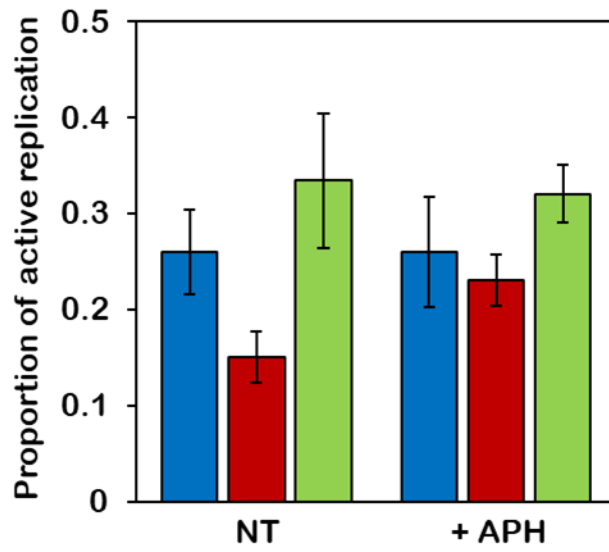
Interestingly, the TD maintained its red:green ratio of 1 and seemed almost unaffected by the APH treatment. When the proportion of DNA that is actually replicating is analyzed (Figure 7B), WT and TD seem to be completely unaffected by the APH treatment while TA actually has a higher proportion of DNA replication following APH treatment. This seemed counterintuitive to us until dormant origin firing was taken into account. When a replication fork stalls, it is common for another origin to fire nearby to complete the replication, this is termed dormant origin firing[35]. So based on the way in which we analyzed the data, this would be counted as having a higher proportion of replicating DNA, when in fact the total amount of DNA replicated would remain static and only the number of origins would change.

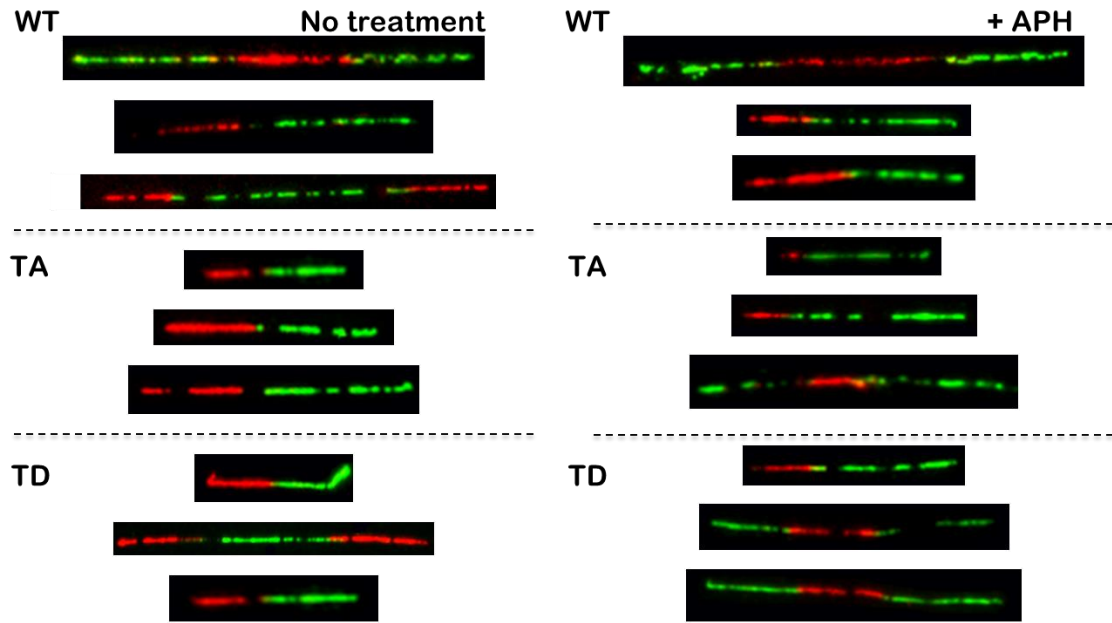
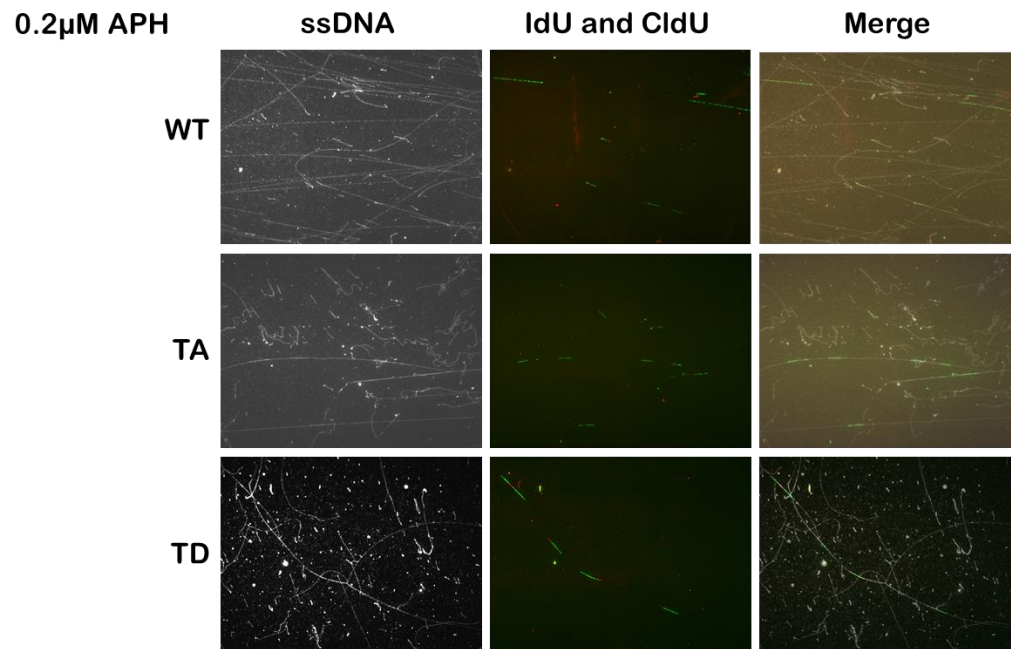
Figure 6 Phosphorylation of FANCD2 facilitates fork restart and stability (A) FA-D2 cells + WT-V5, TA-V5 or TD-V5 were treated with and without .2 μ M APH for 12 hours, then pulsed for 20 minutes with iodouridine (red) followed by a 20 minute pulse with cholouridine (green). The thymidine analogs were stained and visualized. 50 strands were analyzed per condition. (B) The cells were treat as in (A) with the addition of a ssDNA antibody, this will stain every strand of DNA present. The total number strands undergoing active DNA replication, red/green staining, was divided by the total number of DNA strands present. This is preliminary data; at least 100 strands were analyzed per condition. (C) Representative images of strands analyzed per condition per cell type. The first pulse, iodouridine, is in red the second pulse, chlorouridine, is in green. (D) Representative images of ssDNA antibody and IdU/CldU staining with overlays.

A



B



C**D**

Discussion

In this study, we have shown that FANCD2 is extensively phosphorylated during S-phase of the cell cycle. We have also presented data showing that this phosphorylation is DNA damage independent. Both our FANCD2-V5 and FANCD2-3XFLAG immunoprecipitations suggest that a CDK is responsible for this phosphorylation, a result also supported by mass spectrometry.. When we examine the mobility shift that is present when FANCD2 is treated with lambda phosphatase, we see that this shift must be from the hyper-phosphorylation of FANCD2 (a single phosphate weighs ~80 daltons and our phosphate shift is 2-3 kilodaltons). This shift is not present in FANCI even upon the addition of MMC, signifying that FANCD2 is more extensively phosphorylated than FANCI. It has been shown that both FANCD2 and FANCI are phosphorylated by the DNA damage kinases ATM/ATR, this is dependent on DNA damage[13, 14]. Our data suggest that a CDK may also be acting in the pathway to regulate FANCD2 function independent of DNA damage. There is precedent for CDKs phosphorylating DDR protein however it is unique for them to have a DDR protein substrate in the absence of DNA damage.

When the CDK cluster was mutated to alanine (TA mutant) or aspartic acids (TD mutant) we gained insight into the functional significance of these phosphorylations. It appears that phosphorylation at these sites lowers the overall concentration of monoubiquitinated FANCD2 within the cell ,while inhibiting phosphorylation increases monoubiquitination. This is the inverse of FANCI, where phosphorylation has been shown to promote monoubiquitination[16, 18]. The phospho-dead TA mutant was also able to form foci in the absence of damage while the TD mutant was deficient in foci formation even in the presence of DNA damage. We had expected that constitutive monoubiquitination of

FANCD2 may have decreased DNA damage by promoting ICL repair and HR, however, this was not the case. Through chromosomal breakage analysis we see that the TA mutant has higher amounts of damage than either WT or TD and TD had levels of damage slightly lower than WT. When we examined the effects that the mutants had on DNA synthesis, the TA had trouble recovering from APH treatment and appeared to have more active replication occurring, we believe that this is due to dormant origin firing. The TD appeared to be unaffected by damage and continued DNA replication unperturbed.

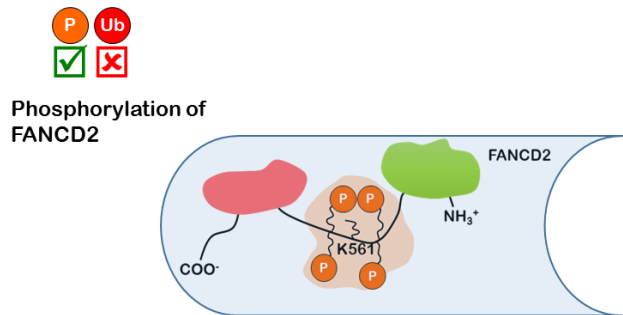
FANCD2 has been shown to be involved in DNA replication in several recent studies[20, 21, 22]. In particular, the recent paper by Madireddy *et al.* highlights the role of FANCD2 in replication across common fragile sites. They state that FANCD2 is important for replication fork stability and efficient replication initiation at these large repeat rich genomic regions[23]. We propose that FANCD2 phosphorylation at these sites acts a “molecular switch” to alter its function from ICL repair to replication fork maintenance. This is supported by both our chromosomal breakage and DNA fiber analysis. Even with high levels of monoubiquitination the TA mutant has extensive chromosomal aberrations and slower fork restart following APH treatment. Since the TA cannot be phosphorylated, it cannot switch roles from ICL to fork maintenance, this results in fork collapse and DNA damage. Upon replication stress it is essential for FANCD2 to be able to switch functions and prevent fork collapse and DNA double strand breaks.

The mechanism by which phosphorylation of this CDK cluster promotes FANCD2’s role in replication fork stability is still under investigation, however, we can speculate as to how it is occurring. One possibility, which has been proposed and studied by other groups, is that FANCD2 arrives at points of instability within the genome, such as CFS, and works

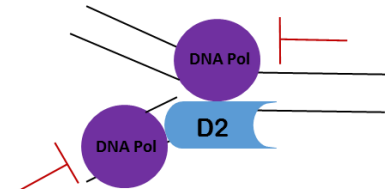
to resolve R-loops at these sites[19, 23]. It is well documented that R-loops occur with a higher frequency during DNA replication and the transcription of genes especially under replication stress; FANCD2 has been shown to resolve R-loops in both murine and human models[19, 36]. Phosphorylation of this CDK cluster may block monoubiquitination of FANCD2 and promote its role in R-loop resolution, which would increase the stability of stressed replication forks. It is also possible that by blocking the monoubiquitination of FANCD2, through phosphorylation, we are allowing FANCD2 to be recruited to replication forks and recruit enzymes that prevent fork collapse. Recent evidence points to fanconi associated nuclease 1 (FAN1) as a candidate for this function. FAN1 has been shown to prevent replication fork progression upon fork collapse, thereby preventing DNA damage, this is a completely separate function from its roles in ICL repair[9, 37]. It is known that FAN1 associates with FANCD2 at ICLs, a similar association could occur at replication forks to halt the fork upon collapse and prevent any DNA damage.

Our mutants will be key in picking apart the mechanism and function of this novel CDK cluster within FANCD2. We still need to do further analysis to answer some key questions such as 1) Does this phosphorylation inhibit FANCD2 monoubiquitination or promote its deubiquitination? 2) Which CDK is responsible for this phosphorylation? 3) How does this phosphorylation promote fork restart and prevent chromosomal aberrations? Given that CDK inhibitors are in clinical use and that over 90% of FA patients are deficient in FANCD2 monoubiquitination, answering these questions could reveal unexplored treatment opportunities for patients

Figure 7. A model of the effects of FANCD2 phosphorylation. This model illustrates the effects on FANCD2 function following phosphorylation of this putative CDK cluster. Upon phosphorylation, left panel, FANCD2 cannot be monoubiquitinated. This promotes its recruitment to stalled replication forks, depicted with red bars, and either through R-loop resolution or FAN1 recruitment the fork is restarted, depicted with green arrows. If FANCD2 is not phosphorylated, right panel, then it will go forward with its canonical function in ICL.

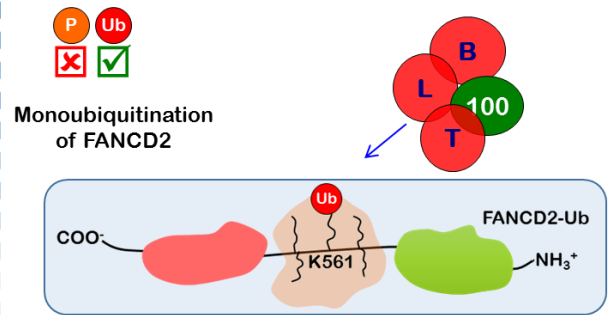
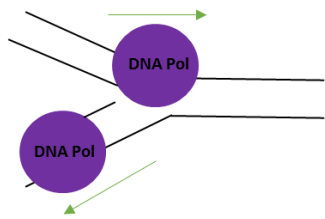


Localization to Stalled Replication Fork

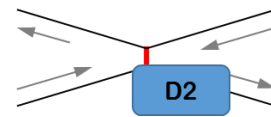


Resolution of R-loops?
FAN1 Recruitment?

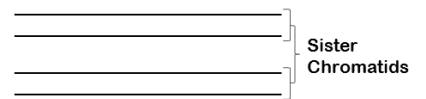
Fork Restart



Localization to ICL



ICL Resolution



Plasmids, site-directed mutagenesis, and transient transfections

The full length *FANCD2* cDNA sequences were TOPO cloned into the pENTR/D-TOPO (Invitrogen) entry vector, and subsequently recombined into the pLenti6.2/V5-DEST (Invitrogen) destination vector and used to generate lentivirus for the generation of stable cell lines. The *TA* and *TD* cDNA were generated by site-directed mutagenesis of the wild type *FANCD2* cDNA using the Quikchange Site-directed Mutagenesis Kit (Stratagene).

The forward and reverse oligonucleotide sequences used are as follows: TA: S726A-FP 5'-AGGCCAAAAATTGGTGGCTCCGCTGTGCCTGGC-3', S624A-FP 5'-TCCTGCAGTGAGCAGGCTCCTCAGGCCTCTGCAC-3', S525A-FP 5'-CTGGATAACATAGCCCCTCAGCAAATACGAAAACCTCTTCTATGTTCTCAGCAC-3'; S726A-RP 5'-GCCAGGCACAGCGGAGCCACCAATTTTTGGCCT-3', S624A-RP 5'-GTGCAGAGGCCTGAGGAGCCTGCTCACTGCAGGA-3', S525A-RP 5'-GTGCTGAGAACATAGAAGAGTTTTTCGTATTTGCTGAGGGGCTATGTTATCCAG-3'. TD: S726D-FP 5'-AGGCCAAAAATTGGTGGATCCGCTGTGCCTGGC-3', S624D-FP 5'-TCCTGCAGTGAGCAGGATCCTCAGGCCTCTGCAC-3', S525D-FP 5'-CTGGATAACATAGACCCTCAGCAAATACGAAAACCTCTTCTATGTTCTCAGCAC-3'; S726D-RP 5'-GCCAGGCACAGCGGATCCACCAATTTTTGGCCT-3', S624D-RP 5'-GTGCAGAGGCCTGAGGATCCTGCTCACTGCAGGA-3', S525D-RP 5'-GTGCTGAGAACATAGAAGAGTTTTTCGTATTTGCTGAGGGTCTATGTTATCCAG-3'.

Lambda phosphatase assay

Cells were harvested and pellets were split into two, lysed in either lambda phosphatase lysis buffer (50 mM Tris-HCl pH 7.5, 150 mM NaCl, 0.1 mM EGTA, 1 mM dithiothreitol, 2 mM MnCl₂, 0.01% Brij35, 0.5% NP-40, and protease inhibitor) or lambda phosphatase buffer with the addition of phosphatase inhibitors, 2 mM Na₃VO₄ and 5 mM NaF for 15 min at 4°C followed by sonication for 10 s at 10% amplitude using a Fisher Scientific Model 500 Ultrasonic Dismembrator. Whole-cell lysates were incubated with or without 30 U of lambda phosphatase 2 h at 30°C, or for the times indicated. Proteins were resolved on NuPage 3-8% w/v Tris-Acetate, 4-12% w/v Bis-Tris gels (Invitrogen), or 6% SuperSep Phos-tag (Wako Pure Chemical Industries) and transferred to polyvinylidene difluoride (PVDF) membranes. Larger proteins were resolved for 5 h on ice.

Cell-cycle synchronization

HeLa cells or the indicated mutants were synchronized by double thymidine block method. Cells were treated with 2.5 mM thymidine for 18 hours, thymidine-free media for 10 hours, and 2.5 mM thymidine for 18 hours to arrest the cell cycle at G₁/S. Cells were washed twice with phosphate-buffered saline (PBS) and released in DMEM + 12% FBS, L-glutamine, and penicillin/streptomycin and analyzed at various time intervals by lambda phosphatase assay and immunoblotting, or flow cytometry

Immunoprecipitation

FA-D2 + LacZ, FA-D2 + FANCD2-V5, U2OS, and U2OS 3XFLAG FANCD2 cells were lysed in Triton-X lysis buffer (50 mM Tris.HCl pH 7.5, 1% v/v Triton X-100, 200 mM

NaCl, 5mM EDTA, 2mM Na₃O₄V, Protease inhibitors (Roche), and 0.153g B-glycerophosphate) on ice for 15 min followed by sonication for 10 s at 10% amplitude using a Fisher Scientific Model 500 Ultrasonic Dismembrator. V5 or FLAG-agarose were washed and blocked with NETN100 (20 mM Tris-HCl pH 7.5, 0.1% NP-40, 100 mM NaCl, 1 mM EDTA, 1 mM Na₃O₄V, 1 mM NaF, protease inhibitor (Roche)) + 1% BSA and the final wash and resuspension was done in Triton-X lysis buffer. Lysate was then incubated with appropriate agarose at 4°C for 2 h, nutating. Beads were then washed in Triton-X lysis buffer and boiled in 1× NuPAGE buffer (Invitrogen) and analyzed for the presence of proteins by SDS-PAGE and immunoblotting or stained using Colloidal Blue Staining Kit (Invitrogen) for mass spectrometry.

Antibodies and immunoblotting

For immunoblotting analysis, cell pellets were washed in PBS and lysed in 2% w/v SDS, 50 mM Tris-HCl, 10 mM EDTA followed by sonication for 10 s at 10% amplitude using a Fisher Scientific Model 500 Ultrasonic Dismembrator. Proteins were resolved on NuPage 3-8% w/v Tris-Acetate or 4-12% w/v Bis-Tris gels (Invitrogen) and transferred to polyvinylidene difluoride (PVDF) membranes. The following antibodies were used: rabbit polyclonal antisera against FANCD2 (NB100-182; Novus Biologicals), FANCI (A301-254A, Bethyl), and pS CDK (9477, Cell Signaling), RPA (NA18, Calbiochem), FLAG (F7425, Sigma), and mouse monoclonal sera against α -tubulin (MS-581-PO, Neomarkers), cyclin A (SC751, Santa Cruz), and V5 (13202, Cell Signaling).

Cell culture

HeLa, U2OS, U2OS 3X FLAG FANCD2 cells were grown in Dulbecco's modified Eagle's medium (DMEM) supplemented with 12% v/v FBS, L-glutamine and

penicillin/streptomycin. 066 and PD7L cells were grown in Roswell Park Memorial Institute medium (RPMI) supplemented with 18% v/v FBS, L-glutamine and penicillin/streptomycin. 293FT viral producer cells (Invitrogen) were cultured in DMEM containing 12% v/v FBS, 0.1 mM non-essential amino acids (NEAA), 1% v/v L-glutamine, 1 mM sodium pyruvate and 1% v/v penicillin/streptomycin. PD20 FA-D2 (*FANCD2*^{hy/-}) cells were purchased from Coriell Cell Repositories (Catalog ID GM16633). These cells harbor a maternally inherited A-G change at nucleotide 376 that leads to the production of a severely truncated protein, and a paternally inherited missense hypomorphic (^{hy}) mutation leading to a R1236H change [38]. To generate stable lines expressing wild type or mutant *FANCD2*, FA-D2 cells were infected with pLenti6.2-*FANCD2* (Invitrogen) lentivirus, followed by selection in DMEM supplemented with 15% v/v FBS, L-glutamine, penicillin/streptomycin and 2 µg/ml blasticidin.

Immunofluorescence microscopy

For immunofluorescence microscopy (IF) analysis, cells were seeded in 4-well tissue culture slides (BD Falcon) in the presence or absence of drug(s) for 24 h. Soluble cellular proteins were pre-permeabilized with 0.3% v/v Triton X-100 and cells were fixed in 4% w/v paraformaldehyde and 2% w/v sucrose at 4°C followed by permeabilization in 0.3% v/v Triton X-100 in PBS. Fixed cells were blocked for 30 minutes in antibody dilution buffer (5% v/v goat serum, 0.1% v/v NP-40, in PBS) and incubated with primary antibody for 1 h. Cells were washed three times in PBS, as well as permeabilization buffer, and incubated for 30 min at room temperature with an Alexa Fluor 488-conjugated or Alexa Fluor 594 secondary antibody and the slides were counterstained and mounted in vectashield plus 4',6-diamidino-2-phenylindole dihydrochloride (DAPI) (Vector

Laboratories). Nuclear foci were scored using a Zeiss AxioImager.A1 upright epifluorescence microscope with AxioVision LE 4.6 image acquisition software. Primary antibodies used for IF were anti-v5 (18870-01; QED Biosciences Inc.), anti-FANCI (A300-212A; Bethyl Laboratories). Statistical significance was determined using paired two-tailed Student's *t*-test analysis.

Chromosome breakage

For chromosome breakage assays, cells were incubated in the absence or presence of .4 μ M APH for 18-24 h. Prior to harvesting, cells were treated with 0.1 μ g/ml Colcemid (Gibco/Invitrogen) for 2 h. Cell pellets were incubated in 0.075 M KCl at 37°C for 18 min, followed by fixation in Carnoy's fixative (3:1 methanol:glacial acetic acid) with multiple changes. Cells were dropped onto chilled slides and air-dried prior to staining with 2.5% w/v Giemsa solution (Sigma). Metaphases were analyzed using a Zeiss AxioImager.A1 upright epifluorescent microscope with AxioVision LE 4.6 image acquisition software.

DNA fiber analysis

For chromosome breakage assays, cells were incubated in the absence or presence of .2 μ M APH for 12 h. The APH media was removed and media containing 30 μ M iodouridine(sigma;, this media was removed and the cells were treated with 30 μ M chloropuridine. Cells were harvested pelleted and the total genomic DNA was purified. The DNA was "stretched" on glass silane coated slides (sigma; S4651-72EA) using a Corning cover glass. The coverslip was then treated with three primary antibodies, against iodouridine, chlorouridine and a ssDNA antibody. A secondary antibody with an attached fluorophore was used against each primary. These slides were mounted using

VECTASHIELD Antifade mounting medium (Vector labs: H-1200). These were then visualized on a Zeiss fluorescence to monitor IdU/CldU nucleoside incorporation.

Works Cited

1. Bogliolo, M., et al., *Mutations in ERCC4, encoding the DNA-repair endonuclease XPF, cause Fanconi anemia*. Am J Hum Genet, 2013. **92**(5): p. 800-6.
2. Kashiyama, K., et al., *Malfunction of nuclease ERCC1-XPF results in diverse clinical manifestations and causes Cockayne syndrome, xeroderma pigmentosum, and Fanconi anemia*. Am J Hum Genet, 2013. **92**(5): p. 807-19.
3. Kim, H. and A.D. D'Andrea, *Regulation of DNA cross-link repair by the Fanconi anemia/BRCA pathway*. Genes Dev, 2012. **26**(13): p. 1393-408.
4. Mamrak, N.E., A. Shimamura, and N.G. Howlett, *Recent discoveries in the molecular pathogenesis of the inherited bone marrow failure syndrome Fanconi anemia*. Blood Rev, 2017. **31**(3): p. 93-99.
5. Knies, K., et al., *Biallelic mutations in the ubiquitin ligase RFW3 cause Fanconi anemia*. J Clin Invest, 2017. **127**(8): p. 3013-3027.
6. Garcia-Higuera, I., et al., *Interaction of the Fanconi anemia proteins and BRCA1 in a common pathway*. Molecular Cell, 2001. **7**(2): p. 249-62.
7. Moldovan, G.L. and A.D. D'Andrea, *How the fanconi anemia pathway guards the genome*. Annu Rev Genet, 2009. **43**: p. 223-49.
8. Moldovan, G.L., et al., *DNA polymerase POLN participates in cross-link repair and homologous recombination*. Molecular and Cellular Biology, 2010. **30**(4): p. 1088-96.

9. MacKay, C., et al., *Identification of KIAA1018/FAN1, a DNA repair nuclease recruited to DNA damage by monoubiquitinated FANCD2*. Cell, 2010. **142**(1): p. 65-76.
10. Smogorzewska, A., et al., *Identification of the FANCI protein, a monoubiquitinated FANCD2 paralog required for DNA repair*. Cell, 2007. **129**(2): p. 289-301.
11. Nakanishi, K., et al., *Human Fanconi anemia monoubiquitination pathway promotes homologous DNA repair*. Proc Natl Acad Sci U S A, 2005. **102**(4): p. 1110-5.
12. Shibata, A. and P.A. Jeggo, *DNA double-strand break repair in a cellular context*. Clin Oncol (R Coll Radiol), 2014. **26**(5): p. 243-9.
13. Taniguchi, T., et al., *Convergence of the fanconi anemia and ataxia telangiectasia signaling pathways*. Cell, 2002. **109**(4): p. 459-72.
14. Ho, G.P., et al., *Phosphorylation of FANCD2 on two novel sites is required for mitomycin C resistance*. Molecular and Cellular Biology, 2006. **26**(18): p. 7005-15.
15. Andreassen, P.R., A.D. D'Andrea, and T. Taniguchi, *ATR couples FANCD2 monoubiquitination to the DNA-damage response*. Genes Dev, 2004. **18**(16): p. 1958-63.
16. Ishiai, M., et al., *FANCI phosphorylation functions as a molecular switch to turn on the Fanconi anemia pathway*. Nat Struct Mol Biol, 2008. **15**(11): p. 1138-46.
17. Chen, Y.H., et al., *ATR-mediated phosphorylation of FANCI regulates dormant origin firing in response to replication stress*. Molecular Cell, 2015. **58**(2): p. 323-38.

18. Cheung, R.S., et al., *Ubiquitination-Linked Phosphorylation of the FANCI S/TQ Cluster Contributes to Activation of the Fanconi Anemia I/D2 Complex*. *Cell Rep*, 2017. **19**(12): p. 2432-2440.
19. Garcia-Rubio, M.L., et al., *The Fanconi Anemia Pathway Protects Genome Integrity from R-loops*. *PLoS Genet*, 2015. **11**(11): p. e1005674.
20. Raghunandan, M., et al., *FANCD2, FANCI and BRCA2 cooperate to promote replication fork recovery independently of the Fanconi Anemia core complex*. *Cell Cycle*, 2015. **14**(3): p. 342-53.
21. Zhu, J., et al., *FANCD2 influences replication fork processes and genome stability in response to clustered DSBs*. *Cell Cycle*, 2015. **14**(12): p. 1809-22.
22. Chaudhury, I., et al., *FANCD2 regulates BLM complex functions independently of FANCI to promote replication fork recovery*. *Nucleic Acids Res*, 2013. **41**(13): p. 6444-59.
23. Madireddy, A., et al., *FANCD2 Facilitates Replication through Common Fragile Sites*. *Molecular Cell*, 2016. **64**(2): p. 388-404.
24. Yeo, J.E., et al., *CtIP mediates replication fork recovery in a FANCD2-regulated manner*. *Hum Mol Genet*, 2014. **23**(14): p. 3695-705.
25. Schlacher, K., H. Wu, and M. Jasin, *A distinct replication fork protection pathway connects Fanconi anemia tumor suppressors to RAD51-BRCA1/2*. *Cancer Cell*, 2012. **22**(1): p. 106-16.
26. Nigg, E.A., *Cyclin-dependent protein kinases: key regulators of the eukaryotic cell cycle*. *Bioessays*, 1995. **17**(6): p. 471-80.

27. Falck, J., et al., *CDK targeting of NBS1 promotes DNA-end resection, replication restart and homologous recombination*. EMBO Rep, 2012. **13**(6): p. 561-8.
28. Tomimatsu, N., et al., *Phosphorylation of EXO1 by CDKs 1 and 2 regulates DNA end resection and repair pathway choice*. Nature Communications, 2014. **5**: p. 3561.
29. Wang, H., et al., *The interaction of CtIP and Nbs1 connects CDK and ATM to regulate HR-mediated double-strand break repair*. PLoS Genet, 2013. **9**(2): p. e1003277.
30. Malumbres, M., *Cyclin-dependent kinases*. Genome Biol, 2014. **15**(6): p. 122.
31. Blazek, D., et al., *The Cyclin K/Cdk12 complex maintains genomic stability via regulation of expression of DNA damage response genes*. Genes Dev, 2011. **25**(20): p. 2158-72.
32. Kim, M. and J.M. Kim, *The role of USP1 autocleavage in DNA interstrand crosslink repair*. FEBS Lett, 2016. **590**(3): p. 340-8.
33. Krokan, H., E. Wist, and R.H. Krokan, *APH inhibits DNA synthesis by DNA polymerase alpha and isolated nuclei by a similar mechanism*. Nucleic Acids Res, 1981. **9**(18): p. 4709-19.
34. Lanneaux, J., et al., *[Fanconi anemia in 2012: diagnosis, pediatric follow-up and treatment]*. Arch Pediatr, 2012. **19**(10): p. 1100-9.
35. Yekezare, M., B. Gomez-Gonzalez, and J.F. Diffley, *Controlling DNA replication origins in response to DNA damage - inhibit globally, activate locally*. J Cell Sci, 2013. **126**(Pt 6): p. 1297-306.

36. Hamperl, S. and K.A. Cimprich, *The contribution of co-transcriptional RNA:DNA hybrid structures to DNA damage and genome instability*. DNA Repair (Amst), 2014. **19**: p. 84-94.
37. Chaudhury, I., D.R. Stroik, and A. Sobeck, *FANCD2-controlled chromatin access of the Fanconi-associated nuclease FAN1 is crucial for the recovery of stalled replication forks*. Molecular and Cellular Biology, 2014. **34**(21): p. 3939-54.
38. Timmers, C., et al., *Positional cloning of a novel Fanconi Anemia gene, FANCD2*. Molecular Cell, 2001. **7**: p. 241-248.

Conclusion

Monoubiquitination of FANCD2 is essential for the function of FA-BRCA pathway. It is this activating step that is absent in over 90% of FA patients. Though it is a critical step within the pathway, there are still long standing questions about its function. Why is FANCD2 monoubiquitinated? What is the function of this post translational modification? What purpose does this monoubiquitination serve in ICL repair? These are key questions, the answers to which will provide much needed insight into the pathogenicity of this disease. It is known that FANCD2 is necessary for chromosomal stability and that defects in monoubiquitination inhibit the downstream proteins from completing HR mediated ICL repair. In order to understand the purpose of this monoubiquitination we must first understand the right environment and conditions that facilitate it. This dissertation lays out a framework for this understanding, first examining monoubiquitination at the chromatin level and then at the protein level.

At the chromatin level we attempted to understand what effects changes to chromatin architecture *via* histone modifications would have on the FA-BRCA pathway. To accomplish this we first look at histone methylation, typically resulting in a closed chromatin structure. We found that certain marks, namely H3K27me3, if inhibited had a drastic effect on FANCD2 monoubiquitination. Inhibition of this mark greatly increased FANCD2 monoubiquitination and foci formation in the absence of any DNA damage. This effect was shown to be mediated by the PRC2 component EZH2. Additionally, we performed tests to see if inhibiting the deacetylation of histones, which should open up chromatin, would have the opposite effect. To our surprise, this was not the case. FANCD2 had lower

levels of monoubiquitination in the presence of HDAC inhibitors. This was thought to be because of the biphasic nature of histone acetylation and deacetylation, being rapidly acetylated and deacetylated. These results highlight the importance of the chromatin environment in DNA repair.

At the protein level we looked at FANCD2 phosphorylation. We were able to show that FANCD2 is extensively phosphorylated in a DNA damage independent manner. These phosphorylations were shown to be cell cycle dependent. Through immunoprecipitation studies, it was found that a CDK is mediating this PTM. *In-silico* analysis revealed a putative CDK phospho cluster proximal to the site of monoubiquitination in FANCD2. Upon mutation of this cluster, to either a phospho-dead (TA) or phospho-mimetic (TD) mutant, differences in monoubiquitination levels were observed. The TA was constitutively monoubiquitinated while the TD could not be monoubiquitinated even in the presence of damage. The TA also had high levels of foci formation while the TD was unable to form foci. The TA mutant had large amounts of chromosomal abnormalities and trouble with fork restart following damage, the opposite was true for the TD mutant. It seems as if the phosphorylation of FANCD2 at this CDK cluster is facilitating blocking FANCD2 monoubiquitination and promoting its roles in replication fork stability. This data showed how vital proper timing of monoubiquitination is in DNA repair

This dissertation demonstrates how complicated and multifaceted ICL repair is. Not only do you need to have an accommodating chromatin environment but it is necessary that the protein itself be modified in the right fashion for proper repair to take place

APPENDIX I

Published in Cell Cycle, 2016

A DUB-less step? Tighten up D-loop

David Vierra*, Karissa L Paquin* , and Niall G.Howlett¹

Department of cell and Molecular Biology, University of Rhode Island, Kingston, RI, USA

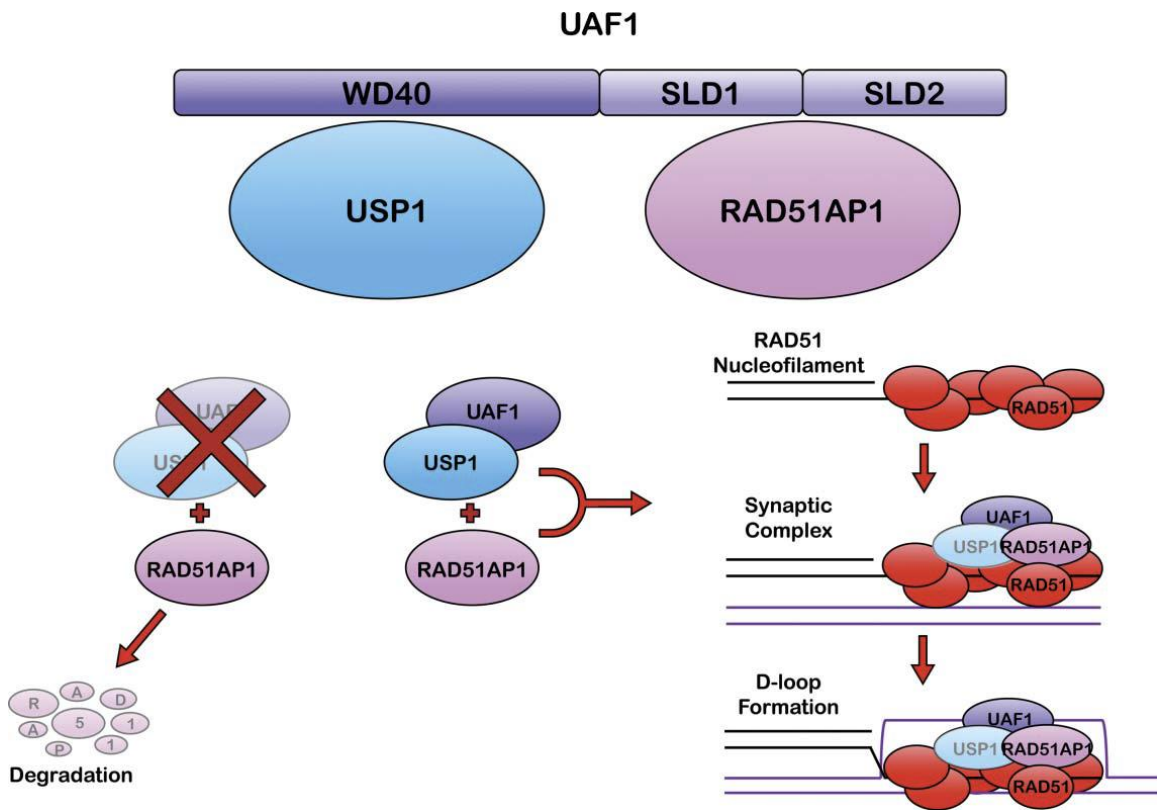
Department of Cell and Molecular Biology, University of Rhode Island, Kingston, Rhode Island, U.S.A

*These authors equally contributed to this work

¹ Corresponding author: Niall G Howlett Ph.D., 379 Center for Biotechnology and Life Sciences, 120 Flagg Road, Kingston, RI, USA, Tel.:+1 401 874 4306; Fax: +1 401 874 2065; Email address: nhowlett@uri.edu

DNA double-strand breaks (DSBs) can arise through exposure to exogenous DNA damaging agents such as ionizing radiation, as well as through endogenous means; for example, via DNA replication fork collapse. Irrespective of the source, the physical severing of the sugar-phosphate backbone represents an acute threat to organismal viability and genome stability. Hanahan and Weinberg describe genome instability and mutation as an enabling characteristic of cancer.¹ Indeed, chromosome structural rearrangements, which are pervasive in cancer, invariably arise from DSB repair gone awry. To deal with this threat, all cells have evolved 2 principal means to repair DSBs: homologous recombination (HR) and nonhomologous DNA end joining (NHEJ). HR is predominantly a conservative and error-free process, employing a homologous template, usually the sister chromatid, to repair the break. RAD51, the eukaryotic ortholog of bacterial RecA, is the major HR protein. Conversely, NHEJ is typically error-prone, and rejoins the break without regard for the state of the ends, often resulting in loss of nucleotides or the re-joining of noncontiguous ends. Exemplifying the importance of HR, many key tumor suppressor genes encode central HR players, e.g. BRCA1 and BRCA2. Furthermore, several genetic diseases characterized by increased cancer risk are caused by mutations in HR genes, one example of which is Fanconi anemia (FA). FA is clinically characterized by congenital defects, bone marrow failure, and increased cancer risk.² FA is caused by mutation of any one of 20 known genes, which encode proteins that function cooperatively in the FA-BRCA pathway to promote HR.³ The molecular links between FA and HR are an area of active investigation. Evidence presented in this volume of *Cell Cycle* points to a novel noncanonical connection between enzymes involved in the major regulatory step of the FA-BRCA pathway and a key HR effector.⁴ This regulatory step is the site-specific monoubiquitination of the FANCD2 and FANCI proteins. The E2 ubiquitin-conjugating enzyme FANCT/UBE2T and the E3 ubiquitin ligase FANCL catalyze the forward step of this reaction. The reverse step - deubiquitination - is catalyzed by the USP1 deubiquitinating enzyme (DUB) and its heterodimeric

Figure 1. Speculative schematic of the role of the USP1-UAF1-RAD51AP1 complex in HR. UAF1 binds to USP1 through its WD40 domain, and RAD51AP1 through its SLD1/2 domains. In the absence of either UAF1 or USP1, RAD51AP1 is degraded by the proteasome. Following RAD51 nucleofilament formation, RAD51AP1 is required for synaptic complex and D-loop formation. This is promoted by the presence of UAF1, however the role of USP1 in this process remains unclear. On the right side of this figure, USP1 is depicted in gray font to signify its uncertain role in this process.



binding partner UAF1.^{5,6} In a large-scale global proteomic screen of DUB-interacting networks, Sowa et al. previously determined that the USP1- UAF1 heterodimer interacts with the RAD51AP1 protein.⁷ RAD51AP1 is a vertebrate specific accessory factor for RAD51 that promotes the assembly of the synaptic complex and D (displacement)-loop, key HR intermediate structures (Fig. 1). However, the functional significance of this interaction was not examined. In the accompanying Cell Cycle manuscript, Cukras et al. have tackled this important question.⁴ The authors verified this interaction and, by depleting UAF1 using siRNA, established that the interaction between USP1 and RAD51AP1 is UAF1-dependent. The authors also established that the UAF1 WD40 repeats as well as its SUMO-like domains (SLDs) are necessary for RAD51AP1 binding. Previous studies had demonstrated that USP1 regulates the stability of the ID (inhibitor of DNA binding) proteins. Similarly, Cukras et al. show that depletion of USP1 or UAF1 leads to destabilization of RAD51AP1. Cukras et al. next sought to map the region of RAD51AP1 that binds to UAF1. Serial truncations and mutagenesis analysis established that residues D133-L137 are required for efficient RAD51AP1-UAF1 binding. Accordingly, deletion of this UAF1 binding region (DDYLDL) resulted in decreased RAD51AP1 stability, supporting the theory that USP1-UAF1-RAD51AP1 form a stable protein complex. Interestingly, mutation of RAD51AP1 K139, previously shown to be a site of ubiquitination, did not affect interaction with UAF1. To explore the functional significance of the RAD51AP1-UAF1 interaction, Cukras et al. expressed wild type or RAD51AP1-DDYLDL in U2OS cells depleted of endogenous RAD51AP1. In contrast to wild type RAD51AP1, the DDYLDL mutant failed to correct cellular ICL sensitivity. Furthermore, RAD51AP1-DDYLDL expressing cells exhibited persistent DNA damage-inducible RAD51 nuclear foci, suggesting that the USP1-UAF1-RAD51AP1 complex may promote the efficient and timely resolution of a key HR intermediate structure. A recent complementary study in Cell Reports by Liang et al. provides further insight into the functional significance of the RAD51AP1-UAF1 interaction.⁸ Similar to Cukras et al., Liang et al. establish that the UAF1 SLDs mediate interaction with RAD51AP1. While mutation of these SLDs compromises interaction with RAD51AP1, these

mutants are proficient for interaction with USP1 and stimulation of its DUB activity toward FANCD2. Importantly, Liang et al. also establish that UAF1 alone stimulates the ability of RAD51AP1 to promote synaptic complex and D-loop formation in vitro, and this stimulation depends on the formation of the RAD51AP1-UAF1 complex. These assays indicate that UAF1-stimulated RAD51AP1 activity is largely USP1-independent. While Cukras et al. clearly show that USP1 forms a complex with UAF1 and RAD51AP1, a role for enzymatic deubiquitination has not been established. Taken together, these studies reveal a novel and critical function for UAF1 in promoting HR that appears to be independent of USP1 deubiquitinating activity. However, it remains to be determined how RAD51AP1 is removed from RAD51 nucleoprotein filaments enabling the dissolution of HR intermediates – ubiquitination remains a plausible mechanism. In conclusion, these studies uncover important mechanistic insight into the molecular biology of HR and FA and suggest the existence of more FA genes linked to the regulation of RAD51 function.

Disclosure of potential conflicts of interest

No potential conflicts of interest were disclosed.

Funding

This work was supported by National Institutes of Health/National Heart, Lung and Blood Institute grant R01HL101977 to NGH, and Rhode Island IDeA Network of Biomedical Research Excellence (RI-INBRE) grant P20GM103430 from the National Institute of General Medical Sciences.

References

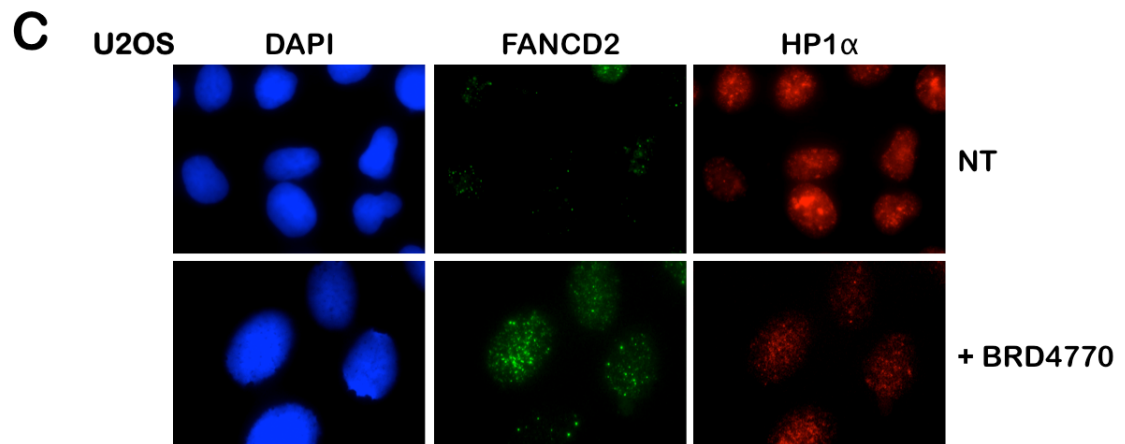
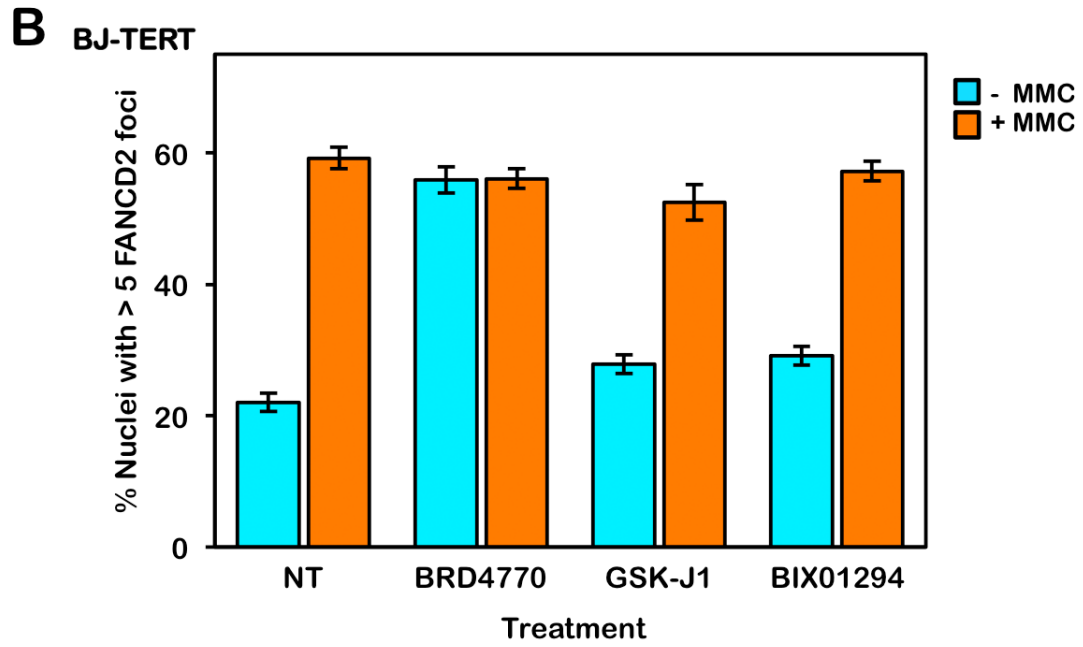
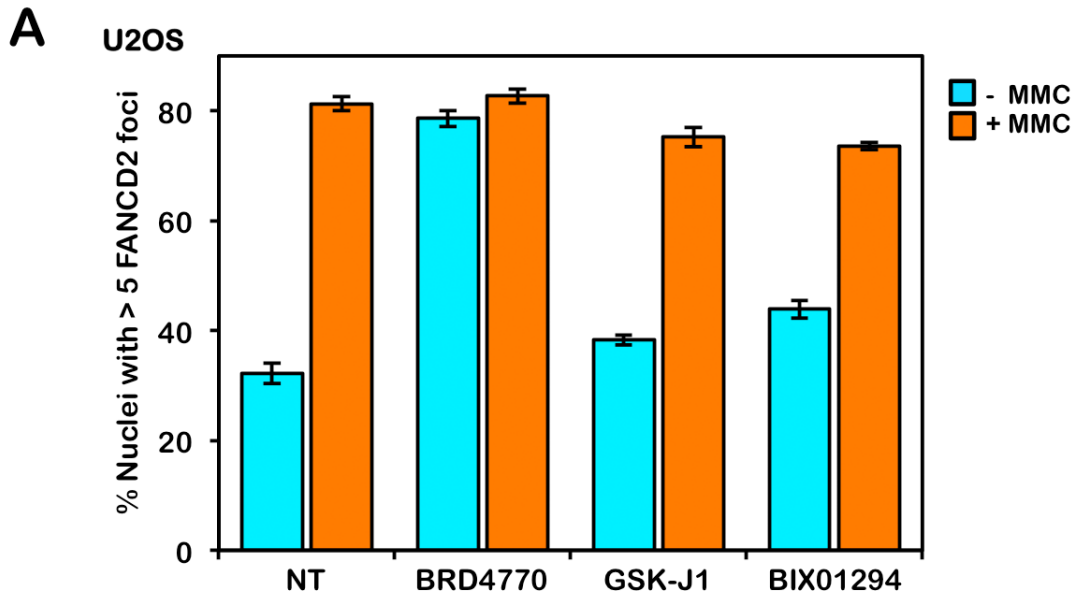
- [1] Hanahan D, Weinberg RA. Hallmarks of cancer: the next generation. *Cell* 2011; 144:646-74; PMID:21376230; <http://dx.doi.org/10.1016/j.cell.2011.02.013>
- [2] Fund FAR. Fanconi anemia: guidelines for diagnosis and management. 4th ed. Eugene, OR: Fanconi Anemia Research Fund; 2014;1-429.
- [3] Walden H, Deans AJ. The Fanconi anemia DNA repair pathway: structural and functional insights into a complex disorder. *Annu Rev Biophys* 2014; 43:257-78; PMID:24773018; <http://dx.doi.org/10.1146/annurev-biophys-051013-022737>
- [4] Cukras S, Lee E, Palumbo P, Benavidez P, Moldovan GL, Kee Y. The USP1-UAF1 complex interacts with RAD51AP1 to promote homologous recombination repair. *Cell Cycle* 2016; 15(19):2636-2646; PMID:27463890; <http://dx.doi.org/10.1080/15384101.2016.1209613>
- [5] Cohn MA, Kowal P, Yang K, Haas W, Huang TT, Gygi SP, D'Andrea AD. A UAF1 containing multisubunit protein complex regulates the Fanconi anemia pathway. *Mol Cell* 2007; 28:786-97; PMID:18082604; <http://dx.doi.org/10.1016/j.molcel.2007.09.031>
- [6] Nijman SM, Huang TT, Dirac AM, Brummelkamp TR, Kerkhoven RM, D'Andrea AD, Bernards R. The deubiquitinating enzyme USP1 regulates the Fanconi anemia pathway. *Mol Cell* 2005; 17:331-9; PMID:15694335; <http://dx.doi.org/10.1016/j.molcel.2005.01.008>
- [7] Sowa ME, Bennett EJ, Gygi SP, Harper JW. Defining the human deubiquitinating enzyme interaction landscape. *Cell* 2009; 138:389-403; PMID:19615732; <http://dx.doi.org/10.1016/j.cell.2009.04.042>

[8] Liang F, Longerich S, Miller AS, Tang C, Buzovetsky O, Xiong Y, Maranon DG, Wiese C, Kupfer GM, Sung P. Promotion of RAD51- mediated homologous DNA pairing by the RAD51AP1-UAF1 complex. Cell Rep 2016; 15:2118-26; PMID:27239033; <http://dx.doi.org/10.1016/j.celrep.2016.05.007>

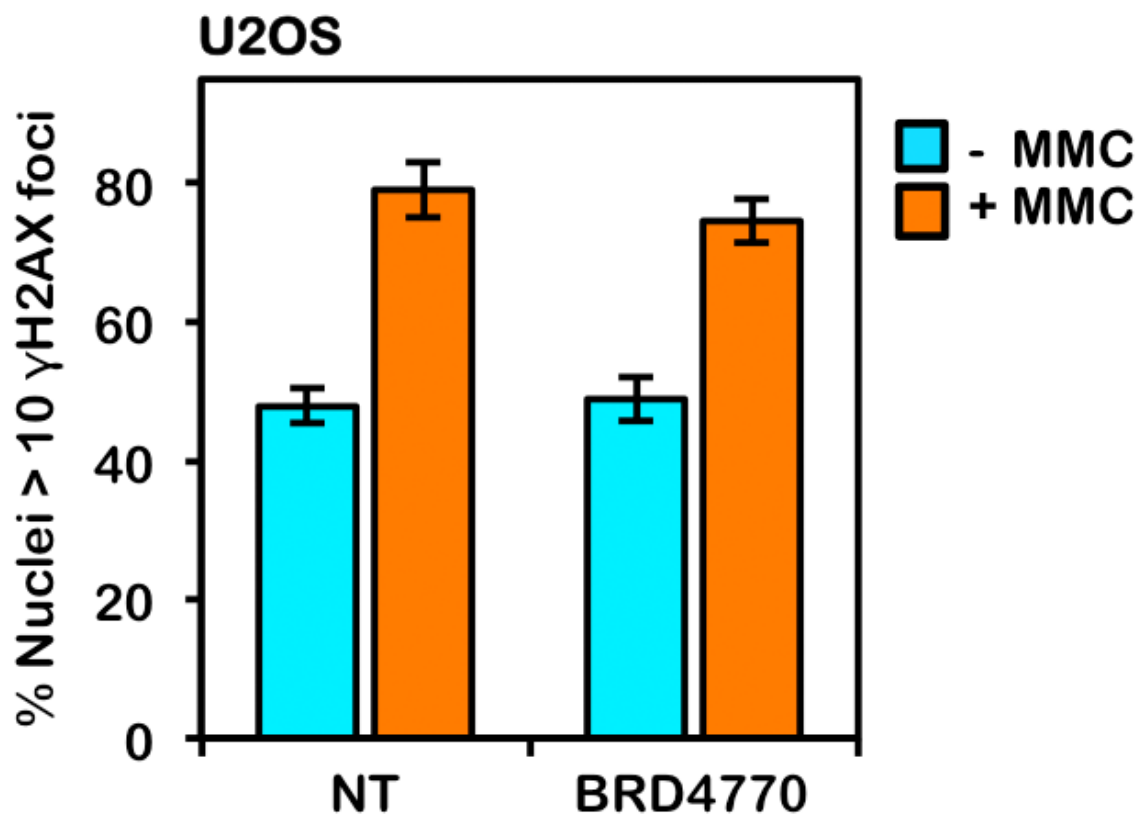
APPENDIX-II

Supplemental information for Manuscript-I “Modulation of the fanconi anemia pathway via chemically induced changes in chromatin structure”

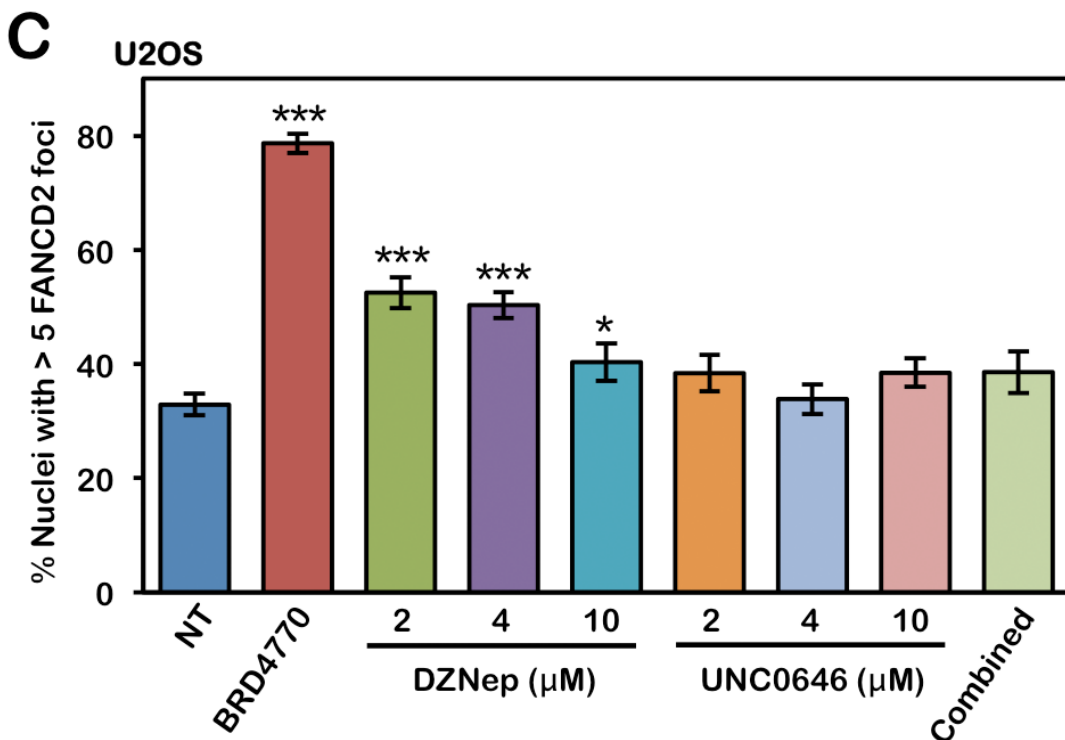
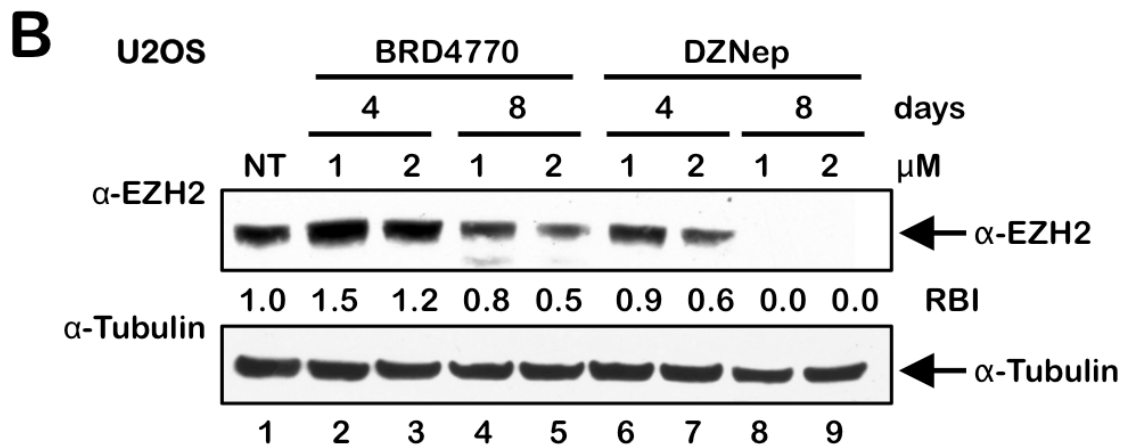
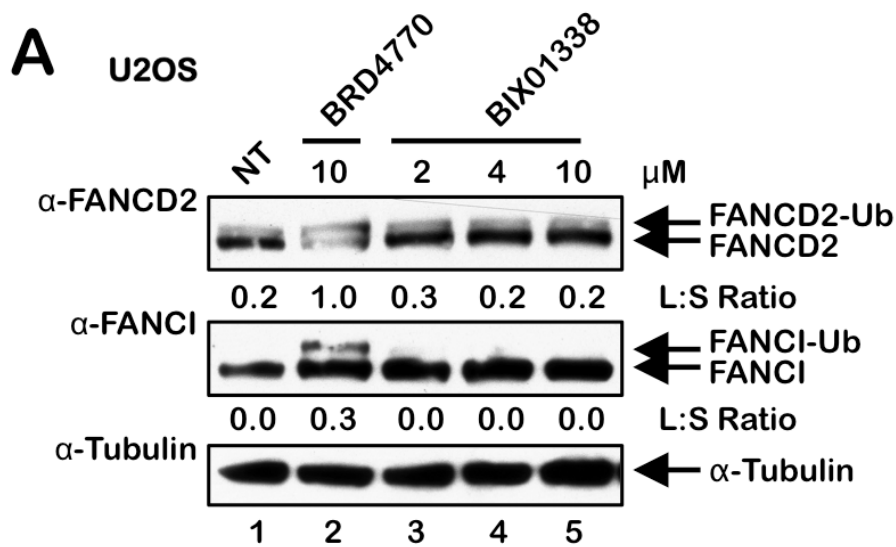
Supplementary Figure 1: The HMTi BRD4770 induces FANCD2 nuclear foci formation. (A) U2OS and (B) BJ-TERT cells were incubated in the absence (NT) or presence of 10 μ M BRD4770, 5 μ M GSK-J1, and 2.5 μ M BIX01294, with (+) and without (-) 200 nM MMC for 24 h. Cells were fixed and stained with rabbit polyclonal anti-FANCD2 antibody (green) and counterstained with DAPI (blue), and the number of nuclei with >5 FANCD2 foci were scored. At least 300 nuclei were scored for each treatment and this experiment was performed at least three times with similar results. Error bars represent the standard errors of the means from three independent experiments. (C) BRD4770 treatment leads to changes in the staining pattern of the heterochromatin marker HP1 α . U2OS cells were incubated in the absence (NT) or presence of 10 μ M BRD4770 for 24 h. Cells were fixed and stained with rabbit polyclonal anti-FANCD2 antibody (green), mouse monoclonal anti-HP1 α antibody (red), and counterstained with DAPI (blue). Representative images from two independent experiments are shown.

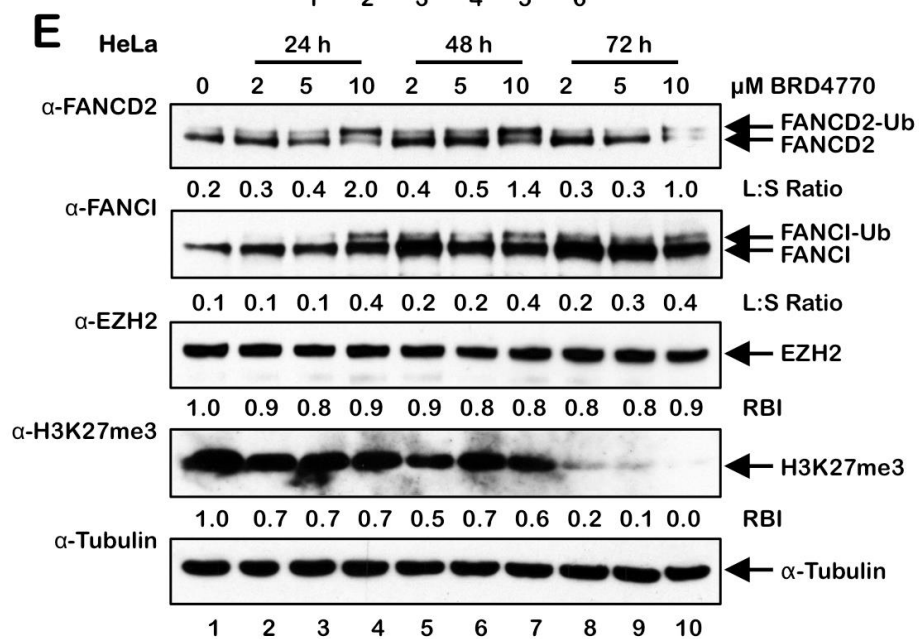
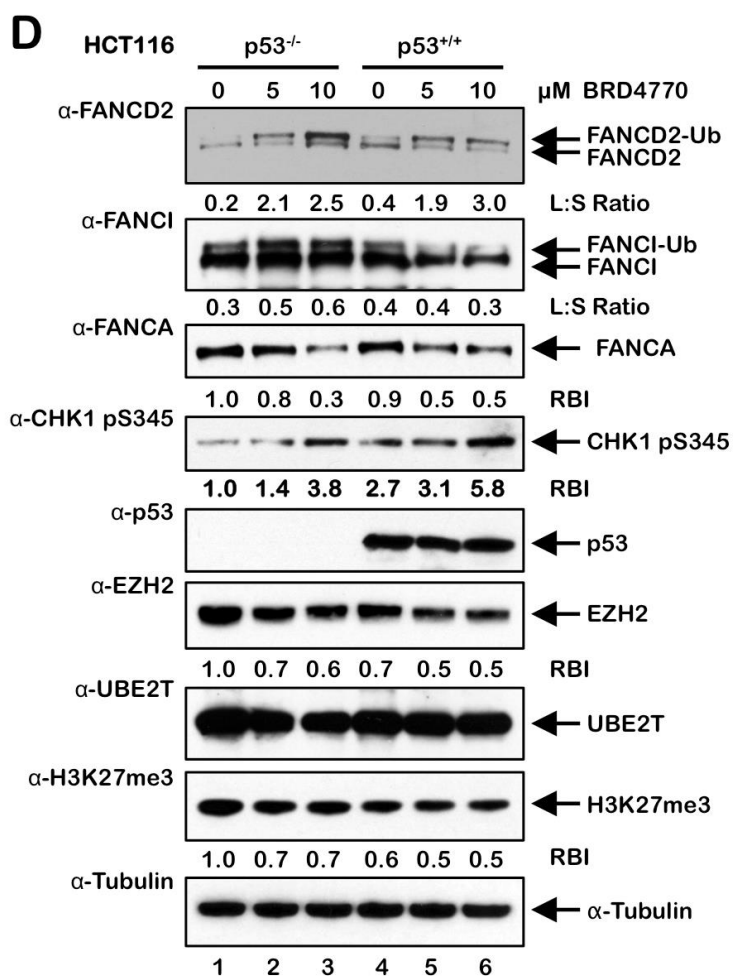


Supplementary Figure 2: BRD4770-induced activation of the FA pathway does not occur *via* the direct induction of DNA damage. U2OS cells were incubated with (+) and without (-) 200 nM mitomycin C (MMC) in the absence (NT) or presence of 10 μ M BRD4770 for 24 h. Cells were fixed and stained with mouse monoclonal anti- γ H2AX antibody and counterstained with DAPI, and the number of nuclei with >10 γ H2AX foci were scored. At least 300 nuclei were scored for each treatment and this experiment was performed three times with similar results. Error bars represent the standard errors of the means from three independent experiments.

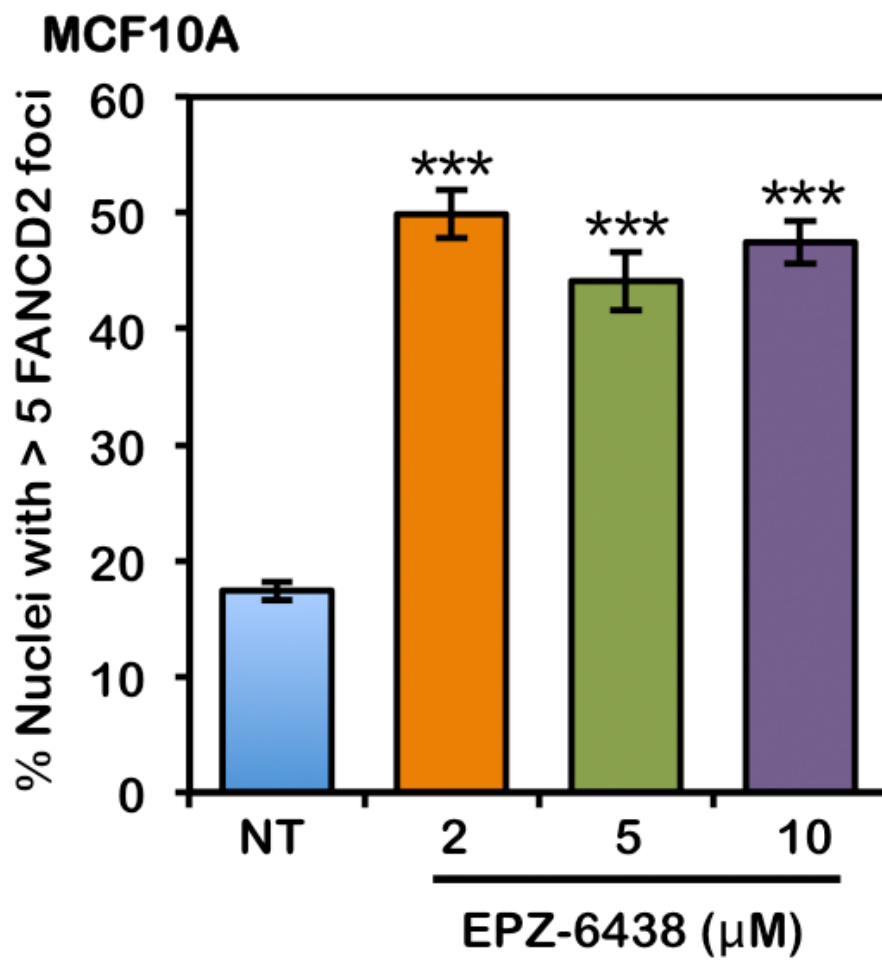


Supplementary Figure 3: BRD4770-induced activation of the FA pathway may occur via inhibition of the PRC2 complex. (A) U2OS cells were incubated in the absence (NT) or presence of the indicated concentrations of BRD4770 or BIX01338 for 24 h. Whole-cell lysates were prepared and immunoblotted with anti-FANCD2, anti-FANCI, and anti- α -Tubulin antibodies. (B) U2OS cells were incubated with the indicated concentrations of BRD4770 and DZNep for 4 and 8 days. Whole-cell lysates were prepared and immunoblotted with anti-EZH2 and anti- α -Tubulin antibodies. L:S Ratio, ratio of monoubiquitinated to nonubiquitinated FANCD2; or FANCI RBI, relative band intensity. (C) U2OS cells were incubated with 10 μ M BRD4770 or the indicated concentrations of DZNep or UNC0646 for 24 h. Cells were fixed and stained with rabbit polyclonal anti-FANCD2 antibody and counterstained with DAPI, and the number of nuclei with >5 FANCD2 foci were scored. At least 300 nuclei were scored for each treatment and this experiment was performed three times with similar results. Error bars represent the standard errors of the means from three independent experiments. *, $P < 0.05$; **, $P < 0.01$; ***, $P < 0.001$, with comparison to untreated cells. (D and E) HCT116 p53^{+/+} and p53^{-/-} (D) and HeLa (E) cells were incubated in the absence or presence of the indicated concentrations of BRD4770 for 24 h (D) or 24, 48, or 72 h (E). Whole-cell lysates were prepared and immunoblotted with the indicated antibodies. L:S Ratio, ratio of monoubiquitinated to nonubiquitinated FANCD2; or FANCI RBI, relative band intensity.

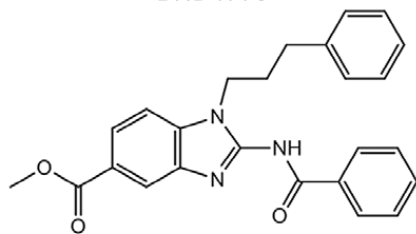
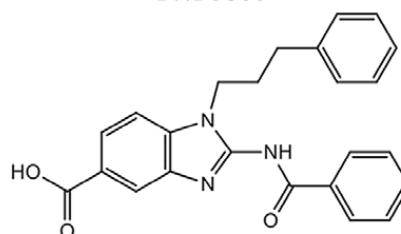
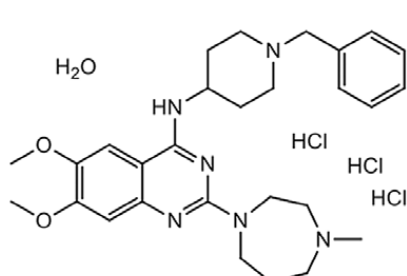
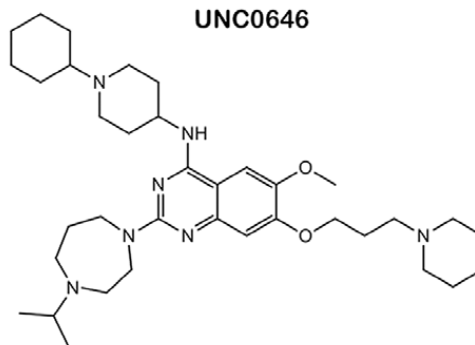
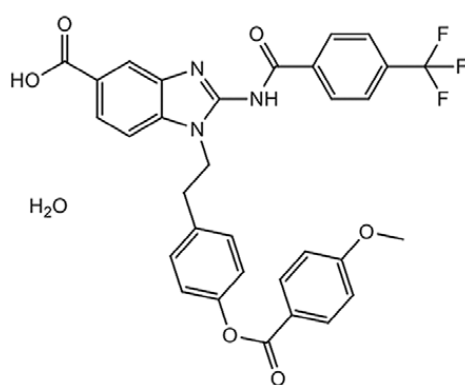
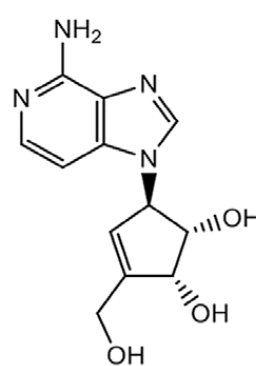
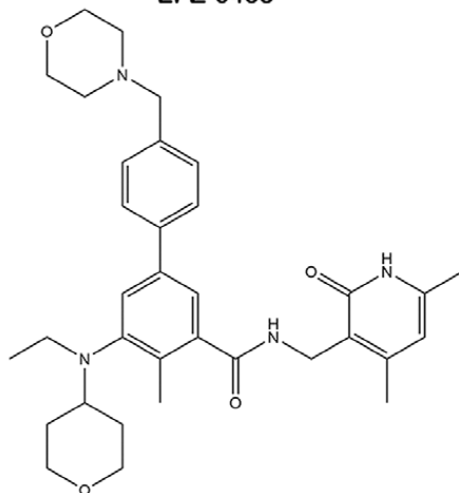




Supplementary Figure 4: Activation of FANCD2 monoubiquitination following treatment with the EZH2 inhibitor EPZ-6438. MCF10A cells were treated with the indicated concentrations of the EZH2-specific inhibitor EPZ-6438 for 24 h. Cells were fixed and stained with rabbit polyclonal anti-FANCD2 antibody and counterstained with DAPI, and the number of nuclei with >5 FANCD2 foci were scored. At least 300 nuclei were scored for each treatment and this experiment was performed twice with similar results. Error bars represent the standard errors of the means from two independent experiments. *** $P < 0.001$, with comparison to untreated cells.

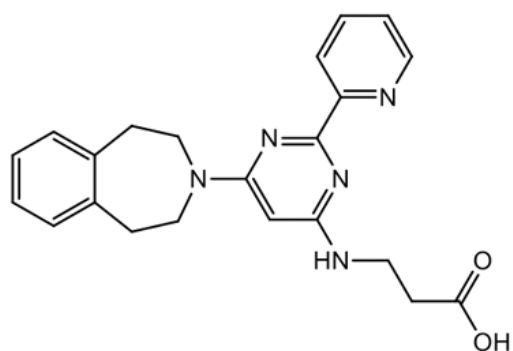


Supplementary Figure 5: Chemical structures of the inhibitors and DNA damaging agents used throughout this study. (A) Histone methyltransferase inhibitors, (B) histone demethylase inhibitors. (C) histone deacetylase inhibitors, and (D) miscellaneous DNA damaging agents.

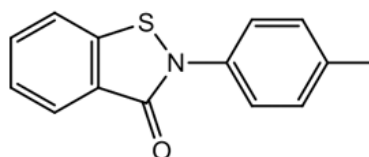
A**Histone Methyltransferase Inhibitors****BRD4770****BRD9539****BIX01294****UNC0646****BIX01338****DZNep****EPZ-6438**

B
Histone Demethylase Inhibitors

GSK-J1

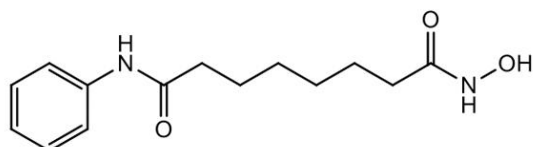


PBIT

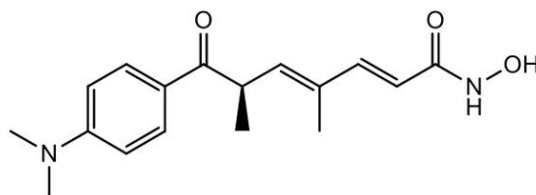


C
Histone Deacetylase Inhibitors

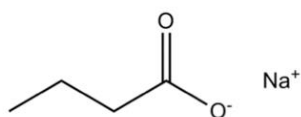
Vorinostat (SAHA)



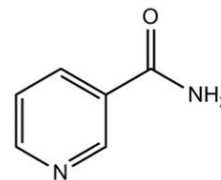
Trichostatin A (TSA)



Sodium Butyrate (NaB)

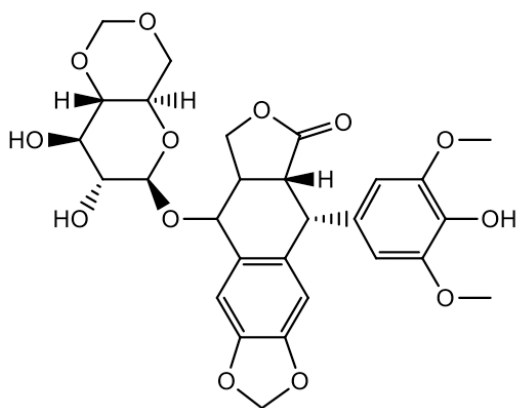


Nicotinamide (NAM)



D
Miscellaneous

Etoposide (VP-16)



Mitomycin C (MMC)

